

Making Sensor Networks Immortal: An Energy-Renewal Approach With Wireless Power Transfer

Liguang Xie, *Student Member, IEEE*, Yi Shi, *Member, IEEE*, Y. Thomas Hou, *Senior Member, IEEE*, and Hanif D. Sherali

Abstract—Wireless sensor networks are constrained by limited battery energy. Thus, finite network lifetime is widely regarded as a fundamental performance bottleneck. Recent breakthrough in the area of wireless power transfer offers the potential of removing this performance bottleneck, i.e., allowing a sensor network to remain operational forever. In this paper, we investigate the operation of a sensor network under this new enabling energy transfer technology. We consider the scenario of a mobile charging vehicle periodically traveling inside the sensor network and charging each sensor node's battery wirelessly. We introduce the concept of renewable energy cycle and offer both necessary and sufficient conditions. We study an optimization problem, with the objective of maximizing the ratio of the wireless charging vehicle (WCV)'s vacation time over the cycle time. For this problem, we prove that the optimal traveling path for the WCV is the shortest Hamiltonian cycle and provide a number of important properties. Subsequently, we develop a near-optimal solution by a piecewise linear approximation technique and prove its performance guarantee.

Index Terms—Lifetime, optimization, wireless power transfer, wireless sensor network (WSN).

I. INTRODUCTION

WIRELESS sensor networks (WSNs) today are mainly powered by batteries. Due to limited energy storage capacity in a battery at each node, a WSN can only remain operational for a limited amount of time. To prolong its lifetime, there have been a flourish of research efforts in the last decade (see, e.g., [3], [6], [10], [26], and [31]). Despite these intensive efforts, the lifetime of a WSN remains a performance bottleneck and is perhaps one of the key factors that hinders its wide-scale deployment.

Although energy-harvesting (or energy-scavenging) techniques (see, e.g., [1], [2], [12], [14], [18], and [21]) were proposed to extract energy from the environment, their success for sensor networks remains limited in practice. This is because

the proper operation of any energy-harvesting technique is heavily dependent on the environment. Furthermore, the size of an energy-harvesting device may pose a concern in deployment, particularly when the size of such a device is of much larger scale than the sensor node that it is attempting to power.

Quite unexpectedly, the recent breakthrough in the area of *wireless power transfer* technology developed by Kurs *et al.* [15] has opened up a revolutionary paradigm for prolonging sensor network lifetime. Basically, Kurs *et al.*'s work showed that by exploiting a novel technique called *magnetic resonant coupling*, wireless power transfer (i.e., the ability to transfer electric power from one storage device to another *without any plugs or wires*) is both feasible and practical. In addition to wireless power transfer, they experimentally showed that the source energy storage device does not need to be in contact with the energy receiving device (e.g., a distance of 2 m) for efficient energy transfer. Moreover, wireless power transfer is immune to the neighboring environment and does not require a line of sight between the power charging and receiving nodes. Recent advances in this technology further show that it can be made portable, with applications to palm size devices such as cell phones [7].

The impact of wireless power transfer on WSNs and other energy-constrained wireless networks is immense. Instead of generating energy locally at a node (as in the case of energy harvesting), one can bring clean electrical energy that is efficiently generated elsewhere to a sensor node periodically and charge its battery without the constraints of wires and plugs. As one can imagine, the applications of wireless power transfer are numerous. For example, wireless power transfer has already been applied to replenish battery energy in medical sensors and implantable devices [34] in the healthcare industry.

Inspired by this new breakthrough in energy transfer technology, this paper reexamines the network lifetime paradigm for a WSN. We envision employing a mobile vehicle carrying a power-charging station to periodically visit each sensor node and charge it wirelessly. This mobile wireless charging vehicle (WCV) can either be manned by a human or be entirely autonomous. In this paper, we investigate the fundamental question of whether such a new technology can be applied to remove the lifetime performance bottleneck of a WSN. That is, through periodic wireless recharge, we show that each sensor node will always have an energy level above a minimum threshold so that the WSN remains operational forever. The main contributions of this paper are as follows.

Manuscript received June 10, 2011; revised December 01, 2011; accepted January 16, 2012; approved by IEEE/ACM TRANSACTIONS ON NETWORKING Editor G. Bianchi. Date of publication February 16, 2012; date of current version December 13, 2012. An abridged version of this paper was presented at the IEEE International Conference on Computer Communications (INFOCOM), Shanghai, China, April 10–15, 2011.

L. Xie, Y. Shi, and Y. T. Hou are with the Bradley Department of Electrical and Computer Engineering, Virginia Tech, Blacksburg, VA 24061 USA (e-mail: xie@vt.edu; yshi@vt.edu; thou@vt.edu).

H. D. Sherali is with the Grado Department of Industrial and Systems Engineering, Virginia Tech, Blacksburg, VA 24061 USA (e-mail: hanifs@vt.edu).

Color versions of one or more of the figures in this paper are available online at <http://ieeexplore.ieee.org>.

Digital Object Identifier 10.1109/TNET.2012.2185831

- We introduce the concept of *renewable energy cycle* where the remaining energy level in a sensor node's battery exhibits some periodicity over a time cycle. We offer both necessary and sufficient conditions for renewable energy cycle and show that feasible solutions satisfying these conditions can offer renewable energy cycles and, thus, unlimited sensor network lifetime.
- We investigate an optimization problem, with the objective of maximizing the ratio of the WCV's vacation time (time spent at its home station) over the cycle time. In terms of achieving the maximum ratio, we prove that the optimal traveling path for the WCV in each renewable cycle is the shortest Hamiltonian cycle. We also derive several interesting properties associated with an optimal solution, such as the optimal objective being independent of traveling direction on the shortest Hamiltonian cycle and the existence of an energy bottleneck node in the network.
- Under the optimal traveling path, our optimization problem now only needs to consider flow routing and the charging time for each sensor node. We formulate an optimization problem for joint flow routing and charging schedule for each sensor node. The problem is shown to be a nonlinear optimization problem and is NP-hard in general. We apply a piecewise linear approximation technique for each nonlinear term and obtain a tight linear relaxation. Based on this linear relaxation, we obtain a feasible solution and prove that it can achieve near-optimality for any desired level of accuracy.

It is worth pointing out that this paper differs fundamentally from the so-called delay-tolerant network (DTN) [13], which can employ various delivery mechanisms such as data MULEs [25] and message ferry [35], among others. It was assumed that a DTN would experience frequent network disconnectivity or partitioning and could tolerate long delays. Both data MULEs and message ferry employ mobile nodes to collect data from sensor nodes when in close range, buffer it, and drop off to remote access points. In essence, the goal of DTN is to exploit intermediate nodes (e.g., mobile nodes) to perform intermittent routing "over time" (i.e., delay tolerant) so as to achieve "eventual delivery." Although the WCV in this paper has some similarity to data MULEs or message ferry, there are some fundamental differences between them. First, a WCV is used for wireless energy charging, not for data collection. Second, network lifetime is not a major concern in the context of DTN, but is the primary concern of our paper. Third, DTN is assumed to tolerate large delays, while we assume real-time data flow from sensor nodes to a base station with negligible delays.

The remainder of this paper is organized as follows. In Section II, we review recent advances in wireless energy transfer technology. In Section III, we describe the scope of our problem for a renewable sensor network. Section IV introduces the concept of renewable energy cycle and presents some interesting properties. Section V shows that an optimal traveling path should be along the shortest Hamiltonian path. In Section VI, we present our problem formulation and a near-optimal solution. Section VII shows how to construct the initial transient cycle preceding the first renewable cycle. In Section VIII, we present numerical results to demonstrate the

properties of a renewable wireless sensor network under our solution. Section IX concludes this paper.

II. WIRELESS POWER TRANSFER: A PRIMER

Efforts of transferring power wirelessly can be dated back to the early 1900s (long before wired electric power grids) when Nikola Tesla experimented with large-scale wireless power distribution [28]. Due to its large electric fields, which is undesirable for efficient power transfer, Tesla's invention was never put into practical use.

Since then, there was hardly any progress in wireless energy transfer for many decades. In the early 1990s, the need of wireless power transfer reemerged when portable electronic devices became widely spread (see, e.g., [30]). The most well-known example is the electric toothbrush. However, due to stringent requirements such as close contact, accurate alignment in charging direction, and uninterrupted line of sight, most of the wireless power transfer technologies at the time (based on inductive coupling) only found limited applications.

Recently, wireless power transfer based on radio frequency (RF) between 850–950 MHz (with a center frequency of 915 MHz) has been explored [23]. Under such radiative energy transfer technology, an RF transmitter broadcasts radio waves in the 915-MHz ISM band, and an RF receiver tunes to the same frequency band to harvest radio power. However, it was found in [17], [22], and [29] that a receiver operating under such radiative energy transfer technology can only obtain about 45 mW power when it is 10 cm away from the RF transmitter, with about 1% power transfer efficiency. A similar experimental finding was reported in [8]. The technology is also sensitive to obstructions between sources and devices, requires complicated tracking mechanisms if relative positions change, and poses more stringent safety concerns. Due to these issues, the potential of RF-based power transfer technology is limited.

The foundation of our work in this paper is based on a recent breakthrough technology by Kurs *et al.* [15], which was published in 2007 and has since caught worldwide attention. In [15], Kurs *et al.* experimentally demonstrated that efficient nonradiative energy transfer was not only possible, but was also practical. They used two magnetic resonant objects having the same resonant frequency to exchange energy efficiently while dissipating relatively little energy in extraneous off-resonant objects. They showed that efficient power transfer implemented in this way can be nearly omnidirectional, irrespective of the environment and even line of sight. The power transfer efficiency, however, decreases with distance. A highlight of their experiment was to fully power a 60-W light bulb from a distance of 2 m away, with about 40% power transfer efficiency.

Since the first demo by Kurs *et al.* in 2007, there has been some rapid advance on wireless energy transfer, particularly in the area of making it portable. In particular, Kurs *et al.* launched a startup company [32], and in 2009, they developed and demonstrated wireless energy transfer for portable devices such as cell phones [7]. Note that the source coil remains sizable, but the device coil is already portable (corresponding to our WCV and sensor node, respectively).

With the recent establishment of the Wireless Power Consortium [33] to set the international standard for interoperable wireless charging, it is expected that wireless power transfer will revolutionize how energy is replenished in the near future.

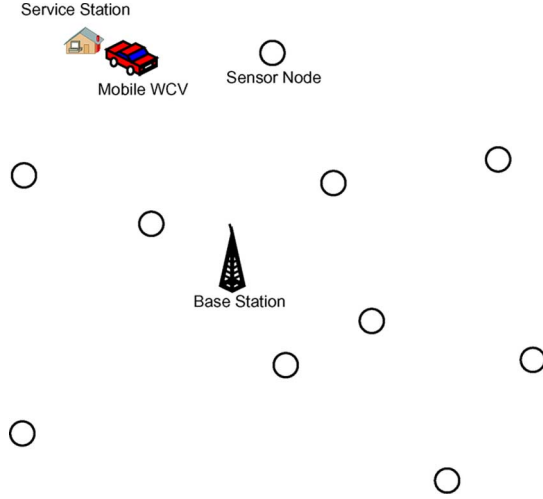


Fig. 1. Example sensor network with a mobile WCV.

III. PROBLEM DESCRIPTION

We consider a set of sensor nodes \mathcal{N} distributed over a two-dimensional area (see Fig. 1). Each sensor node has a battery capacity of E_{\max} and is fully charged initially.¹ Also, denote E_{\min} as the minimum energy at a sensor node battery (for it to be operational). For simplicity, we define network lifetime as the time until the energy level of any sensor node in the network falls below E_{\min} [3], [24], [31].² Although a more general definition of network lifetime (e.g., [5]) is available, we decided to choose a simple network lifetime definition in this paper, which is sufficient to show the potential of wireless energy transfer in a sensor network.

Each sensor node i generates sensing data with a rate of R_i (in bits/second), $i \in \mathcal{N}$. Within the sensor network, there is a fixed base station (B), which is the sink node for all data generated by all sensor nodes. Multihop data routing is employed for forwarding data by the sensor nodes. Denote f_{ij} as the flow rate from sensor node i to sensor node j , and f_{iB} as the flow rate from sensor node i to the base station B , respectively. Then, we have the following flow balance constraint at each sensor node i :

$$\sum_{k \in \mathcal{N}}^{k \neq i} f_{ki} + R_i = \sum_{j \in \mathcal{N}}^{j \neq i} f_{ij} + f_{iB} \quad (i \in \mathcal{N}). \quad (1)$$

Each sensor node consumes energy for data transmission and reception. Denote p_i as the energy consumption rate at sensor node $i \in \mathcal{N}$. In this paper, we use the following power consumption model [3], [10]:

$$p_i = \rho \sum_{k \in \mathcal{N}}^{k \neq i} f_{ki} + \sum_{j \in \mathcal{N}}^{j \neq i} C_{ij} f_{ij} + C_{iB} f_{iB} \quad (i \in \mathcal{N}) \quad (2)$$

where ρ is the energy consumption for receiving one unit of data rate, C_{ij} (or C_{iB}) is the energy consumption for transmitting

¹To simplify the model, we assume that there is no limit on the number of times batteries can be recharged. In practice, rechargeable batteries can be recharged only for a limited number of times. The battery capacity also decreases, and batteries may eventually need to be replaced.

²In the listed references as well as many other references, E_{\min} is typically set to 0.

one unit of data rate from node i to node j (or the base station B). Furthermore, $C_{ij} = \beta_1 + \beta_2 D_{ij}^\alpha$, where D_{ij} is the distance between nodes i and j , β_1 is a distance-independent constant term, β_2 is a coefficient of the distance-dependent term, and α is the path loss index. In the model, $\rho \sum_{k \in \mathcal{N}}^{k \neq i} f_{ki}$ is the energy consumption rate for reception, and $\sum_{j \in \mathcal{N}}^{j \neq i} C_{ij} f_{ij} + C_{iB} f_{iB}$ is the energy consumption rate for transmission.

To recharge the battery at each sensor node, a mobile WCV is employed in the network. The WCV starts from a service station (S), and its traveling speed is V (in meters/second). When it arrives at a sensor node, say i , it will spend τ_i amount of time to charge the sensor node's battery wirelessly via wireless power transfer [15]. Denote U as the energy transfer rate of the WCV. After τ_i , the WCV leaves node i and travels to the next node on its path. We assume that the WCV has sufficient energy to charge all sensor nodes in the network.

After the WCV visits all the sensor nodes in the network, it will return to its service station to be serviced (e.g., replacing or recharging its battery) and get ready for the next tour. We call this resting period *vacation time*, denoted as τ_{vac} . After this vacation, the WCV will go out for its next tour.

Denote τ as the time for a trip cycle of the WCV. A number of important questions need to be addressed for such a network. First and foremost, one would ask whether it is possible to have each sensor node never run out of its energy. If this is possible, then the sensor network will have unlimited lifetime and will never cease to be operational. Second, if the answer to the first question is positive, then is there any optimal plan (including traveling path, stop schedule) such that some useful objective can be maximized or minimized? For example, in this paper, we would like to maximize the percentage of time in a cycle that the WCV spends on its vacation (i.e., $\frac{\tau_{\text{vac}}}{\tau}$), or equivalently, to minimize the percentage of time that the WCV is out in the field.

IV. CONSTRUCTING RENEWABLE CYCLE

In this section, we focus on the renewable cycle construction. We assume that the WCV starts from the service station, visits each sensor node once in a cycle, and ends at the service station (see Fig. 2). Furthermore, we assume that the data flow routing in the network is invariant with time, with both routing and flow rates being part of our optimization problem.

The middle sawtooth graph (in dashed line) in Fig. 3 shows the energy level of a sensor node i during the first two renewable cycles. Note that there is an initialization cycle (marked in the gray area) before the first renewable cycle. That initialization cycle will be constructed in Section VII once we have a solution to the renewable cycles.

Denote $P = (\pi_0, \pi_1, \dots, \pi_N, \pi_0)$ as the physical path traversed by the WCV over a trip cycle, which starts from and ends at the service station (i.e., $\pi_0 = S$), and the i th node traversed by the WCV along path P is π_i , $1 \leq i \leq |\mathcal{N}|$. Denote $D_{\pi_0 \pi_1}$ as the distance between the service station and the first sensor node visited along P and $D_{\pi_k \pi_{k+1}}$ as the distance between the k th and $(k+1)$ th sensor nodes, respectively. Denote a_i as the arrival time of the WCV at node i in the first renewable energy cycle. We have

$$a_{\pi_i} = \tau + \sum_{k=0}^{i-1} \frac{D_{\pi_k \pi_{k+1}}}{V} + \sum_{k=1}^{i-1} \tau_{\pi_k}. \quad (3)$$

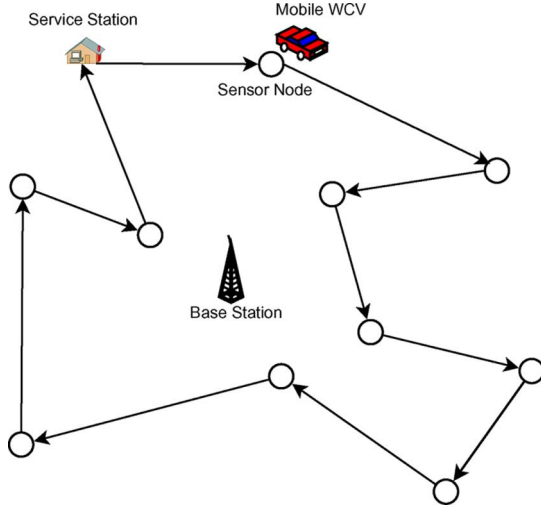


Fig. 2. A WCV periodically visits each sensor node and charges its battery via wireless energy transfer.

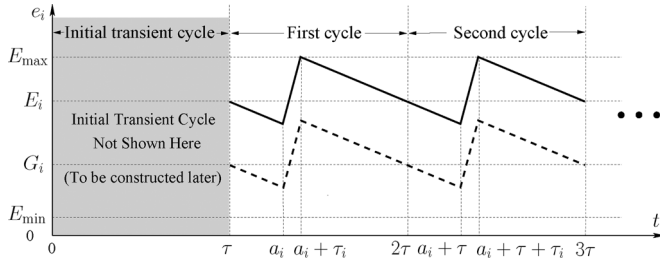


Fig. 3. Energy level of a sensor node i during the first two renewable cycles (partially recharged versus fully recharged).

Denote D_P as the physical distance of path P and $\tau_P = D_P/V$ as the time spent for traveling over distance D_P . Recall that τ_{vac} is the vacation time the WCV spends at its service station. Then, the cycle time τ can be written as

$$\tau = \tau_P + \tau_{\text{vac}} + \sum_{i \in \mathcal{N}} \tau_i \quad (4)$$

where $\sum_{i \in \mathcal{N}} \tau_i$ is the total amount of time the WCV spends near all the sensor nodes in the network for wireless power transfer.

We formally define a renewable energy cycle as follows

Definition 1: The energy level of a sensor node $i \in \mathcal{N}$ exhibits a renewable energy cycle if it meets the following two requirements: (i) it starts and ends with the same energy level over a period of τ ; and (ii) it never falls below E_{\min} .

During a renewable cycle, the amount of charged energy at a sensor node i during τ_i must be equal to the amount of energy consumed in the cycle (so as to ensure the first requirement in Definition 1). That is

$$\tau \cdot p_i = \tau_i \cdot U (i \in \mathcal{N}). \quad (5)$$

Note that when the WCV visits a node i at time a_i during a renewable energy cycle, it does not have to recharge the sensor node's battery to E_{\max} . This is illustrated in Fig. 3, where G_i denotes the starting energy of sensor node i in a renewable cycle and $g_i(t)$ denotes the energy level at time t (dashed sawtooth graph). During a cycle $[\tau, 2\tau]$, we see that the energy level has only two slopes: (i) a slope of $-p_i$ when the WCV is not at this node (i.e., noncharging period), and (ii) a slope of $(U - p_i)$

when the WCV is charging this node at a rate of U (i.e., charging period). It is clear that $g_i(a_i) \leq g_i(t) \leq g_i(a_i + \tau_i)$, i.e., node i 's energy level is lowest at time a_i and is highest at time $a_i + \tau_i$.

Also shown in Fig. 3 is another renewable energy cycle (in solid sawtooth graph) where the battery energy is charged to E_{\max} during a WCV's visit. For this energy curve, denote E_i as the starting energy of node i in a renewable cycle and $e_i(t)$ as the energy level at time t , respectively. Let φ_{Full}^* be an optimal solution with fully recharged batteries in each cycle that maximizes the ratio of the WCV's vacation time over the cycle time. Let φ^* be an optimal solution, where there is no requirement on whether or not a node's battery is fully recharged. Naturally, the optimal objective obtained by φ_{Full}^* is no more than the optimal objective obtained by φ^* due to the additional requirement (batteries are fully recharged) in φ_{Full}^* . Surprisingly, the following lemma shows that φ_{Full}^* is equally good as φ^* in terms of maximizing the ratio of the WCV's vacation time over the cycle time. Thus, for our optimization problem, it is sufficient to consider a solution with fully recharged batteries.

Lemma 1: Solution φ_{Full}^* achieves the same maximum ratio of vacation time to the cycle time as that by solution φ^* .

Proof: Our proof has two parts. (i) First, we show that the maximal ratio of vacation time to the cycle time achieved by solution φ^* is greater than or equal to that achieved by solution φ_{Full}^* . (ii) Second, we show that the converse is also true, i.e., the maximal ratio of vacation time to the cycle time achieved by solution φ_{Full}^* is also greater than or equal to that achieved by solution φ^* . If both (i) and (ii) hold, then the lemma is proved.

Since φ_{Full}^* is an optimal solution with the additional requirement (fully recharged batteries in each cycle), the maximal ratio of vacation time to the cycle time obtained by φ_{Full}^* is no more than that obtained by φ^* . Thus, (i) holds.

We now prove (ii). Instead of considering the optimal solution φ^* , we will prove that any ratio achieved by a feasible solution φ can also be achieved by a feasible fully recharged solution $\hat{\varphi}$. If this is true, in the special case that $\varphi = \varphi^*$ is an optimal solution, we have that the maximal ratio achieved by φ^* can also be achieved by a feasible fully recharged solution. Therefore, (ii) will hold.

The proof is based on construction. Suppose $\varphi = (P, a_i, G_i, f_{ij}, f_{iB}, \tau, \tau_i, \tau_P, \tau_{\text{vac}}, p_i)$ is a feasible solution to our problem. We construct $\hat{\varphi} = (\hat{P}, \hat{a}_i, E_i, \hat{f}_{ij}, \hat{f}_{iB}, \hat{\tau}, \hat{\tau}_i, \hat{\tau}_P, \hat{\tau}_{\text{vac}}, \hat{p}_i)$ by letting $\hat{P} = P$, $\hat{a}_i = a_i$, $E_i = E_{\max} + p_i(a_i + \tau_i - \tau) - U\tau_i$, $\hat{f}_{ij} = f_{ij}$, $\hat{f}_{iB} = f_{iB}$, $\hat{\tau} = \tau$, $\hat{\tau}_i = \tau_i$, $\hat{\tau}_P = \tau_P$, $\hat{\tau}_{\text{vac}} = \tau_{\text{vac}}$, and $\hat{p}_i = p_i$. Note that under $\hat{\varphi}$, the maximal energy level of node i occurs at time $(\hat{a}_i + \hat{\tau}_i)$, which is

$$\begin{aligned} e_i(\hat{a}_i + \hat{\tau}_i) &= E_i + U\hat{\tau}_i - p_i(\hat{a}_i + \hat{\tau}_i - \hat{\tau}) \\ &= [E_{\max} + p_i(a_i + \tau_i - \tau) - U\tau_i] + U\tau_i - p_i(a_i + \tau_i - \tau) \\ &= E_{\max}. \end{aligned}$$

Thus, $\hat{\varphi}$ is a fully recharged solution. Moreover, it is clear that $\frac{\hat{\tau}_{\text{vac}}}{\hat{\tau}} = \frac{\tau_{\text{vac}}}{\tau}$ since $\hat{\tau} = \tau$ and $\hat{\tau}_{\text{vac}} = \tau_{\text{vac}}$. Now, all we need to do is to verify that $\hat{\varphi}$ is a feasible renewable cycle.

To show that $\hat{\varphi}$ is feasible, we need to verify that $\hat{\varphi}$ meets Constraints (1), (2), and (4), as well as $e_i(t) \geq E_{\min}$ for $i \in \mathcal{N}$, $t \geq \tau$. Furthermore, to show that $\hat{\varphi}$ is a renewable cycle, we need to verify that $e_i(k\tau) = E_i$ for $k \in \mathbb{N}$. We now verify each

of these requirements. Since φ is a feasible solution, it satisfies (1), (2), and (4). In $\hat{\varphi}$, we have $\hat{\tau} = \tau$, $\hat{\tau}_i = \tau_i$, $\hat{\tau}_p = \tau_p$, $\hat{\tau}_{vac} = \tau_{vac}$, $\hat{f}_{ij} = f_{ij}$, $\hat{f}_{iB} = f_{iB}$, and $\hat{p}_i = p_i$. Then, $\hat{\varphi}$ also satisfies (1), (2), and (4).

We now show that $e_i(t) \geq E_{min}$ for $i \in \mathcal{N}$, $t \geq \tau$. Since φ is a feasible solution, $E_{max} \geq g_i(a_i + \tau_i) = G_i + U\tau_i - p_i(a_i + \tau_i - \tau)$. Thus, we have $E_{max} + p_i(a_i + \tau_i - \tau) - U\tau_i \geq G_i$. Since E_i is set as $E_i = E_{max} + p_i(a_i + \tau_i - \tau) - U\tau_i$, we have $E_i \geq G_i$. Moreover, since $\hat{p}_i = p_i$, the energy at a node i in $\hat{\varphi}$, $e_i(t)$, is parallel to $g_i(t)$ in φ . Because of this parallelism and $E_i \geq G_i$, we have that $e_i(t) \geq g_i(t)$ for $i \in \mathcal{N}$. Since φ is a feasible solution, we have $g_i(t) \geq E_{min}$ for $i \in \mathcal{N}$. Thus, $e_i(t) \geq g_i(t) \geq E_{min}$ for $i \in \mathcal{N}$. Therefore, $\hat{\varphi}$ is feasible.

Because of the parallelism and $g_i(k\tau) = G_i$ for $k = 1, 2, \dots$, we have $e_i(k\tau) = E_i$ for $k = 1, 2, \dots$. Thus, $\hat{\varphi}$ is a feasible renewable cycle, and (ii) holds. ■

Based on Lemma 1, we will only consider renewable cycles where each node is fully recharged when it is visited by the WCV. Since the energy level at node i is at its lowest at time a_i , to ensure the second requirement in Definition 1, we must have $e_i(a_i) = E_i - (a_i - \tau)p_i \geq E_{min}$. Since for a renewable cycle

$$\begin{aligned} E_i &= e_i(2\tau) = e_i(a_i + \tau_i) - (2\tau - a_i - \tau_i)p_i \\ &= E_{max} - (2\tau - a_i - \tau_i)p_i \end{aligned} \quad (6)$$

we have $e_i(a_i) = E_{max} - (2\tau - a_i - \tau_i)p_i - (a_i - \tau)p_i = E_{max} - (\tau - \tau_i)p_i$. Therefore

$$E_{max} - (\tau - \tau_i) \cdot p_i \geq E_{min} \quad (i \in \mathcal{N}). \quad (7)$$

To construct a renewable energy cycle, we need to consider the traveling path P , the arrival time a_i , the starting energy E_i , the flow rates f_{ij} and f_{iB} , time intervals τ , τ_i , τ_p , and τ_{vac} , and power consumption p_i . By (3) and (6), a_i and E_i are variables that can be derived from P , τ , and τ_i . Thus, a_i and E_i can be excluded from a solution φ . Therefore, we have $\varphi = (P, f_{ij}, f_{iB}, \tau, \tau_i, \tau_p, \tau_{vac}, p_i)$. Although more variables can be removed from φ , we keep this representation for the sake of future discussion.

For a renewable energy cycle, we have the following lemma.

Lemma 2: A cycle is a renewable energy cycle if and only if Constraints (4), (5), and (7) are satisfied at each sensor node $i \in \mathcal{N}$.

Proof: The ‘‘only if’’ part of the lemma can be proved by showing that a renewable cycle meets (4), (5), and (7). This has already been shown in the description of the renewable cycle.

We now prove the ‘‘if’’ part of the lemma, i.e., if (4), (5), and (7) hold, then (i) and (ii) in Definition 1 will also hold, thus the cycle is a renewable energy cycle. Since (4) holds, the given cycle satisfies the time constraint. Constraint (5) ensures that the amount of energy charged to each sensor node i during τ_i is equal to the amount of energy consumed by sensor node i in the cycle. Thus, the energy level at each sensor node i at the end of the cycle is the same as that at the beginning of the cycle. Therefore, requirement (i) in Definition 1 is satisfied.

During the first renewable cycle, the lowest energy level at node i occurs at time a_i , which is

$$\begin{aligned} e_i(a_i) &= e_i(\tau) - (a_i - \tau)p_i = e_i(2\tau) - (a_i - \tau)p_i \\ &= E_{max} - (2\tau - a_i - \tau_i)p_i - (a_i - \tau)p_i \\ &= E_{max} - (\tau - \tau_i)p_i \geq E_{min} \end{aligned}$$

where the second equality holds by requirement (i), which we just proved, the third equality holds by (6), the fourth equality holds by $e_i(a_i + \tau_i) = E_{max}$ in a fully recharged solution, and the last inequality holds by (7). Since the lowest energy level of node i occurs at time a_i and is still no less than E_{min} , requirement (ii) in Definition 1 is satisfied. The proof of the ‘‘if’’ part of the lemma is complete. ■

The following property shows that in an optimal solution, there exists at least one energy ‘‘bottleneck’’ node in the network, where the energy level at this node drops exactly to E_{min} upon the WCV’s arrival.

Property 1: In an optimal solution, there exists at least one node in the network with its battery energy dropping to E_{min} when the WCV arrives at this node.

Proof: The proof is based on contradiction (i.e., if this is not true, then we can further increase the objective value, thus leading to a contradiction).

Suppose that there exists an optimal solution $\varphi^* = (P^*, f_{ij}^*, f_{iB}^*, \tau^*, \tau_i^*, \tau_p^*, \tau_{vac}^*, p_i^*)$ where none of the nodes in the network has its energy level drop to E_{min} , i.e., $e_i^*(t) > E_{min}$ for all $i \in \mathcal{N}$, $t \geq \tau$. Then, we can construct a new solution $\hat{\varphi} = (\hat{P}, \hat{f}_{ij}, \hat{f}_{iB}, \hat{\tau}, \hat{\tau}_i, \hat{\tau}_p, \hat{\tau}_{vac}, \hat{p}_i)$ by choosing $\gamma = \min_{i \in \mathcal{N}} \left\{ \frac{E_{max} - E_{min}}{(\tau^* - \tau_i^*)p_i^*} \right\} - 1$ and letting $\hat{P} = P^*$, $\hat{f}_{ij} = f_{ij}^*$, $\hat{f}_{iB} = f_{iB}^*$, $\hat{\tau} = (1 + \gamma)\tau^*$, $\hat{\tau}_i = (1 + \gamma)\tau_i^*$, $\hat{\tau}_p = \tau_p^*$, $\hat{\tau}_{vac} = \tau_{vac}^* + \gamma(\tau^* - \sum_{i \in \mathcal{N}} \tau_i^*)$, and $\hat{p}_i = p_i^*$.

Now, we show that $\gamma > 0$. Since $e_i^*(t) > E_{min}$ for all $i \in \mathcal{N}$, $t \geq \tau$, we have $e_i^*(a_i) = E_{max} - (\tau^* - \tau_i^*)p_i^* > E_{min}$ for all $i \in \mathcal{N}$, i.e., $\min_{i \in \mathcal{N}} \{E_{max} - (\tau^* - \tau_i^*)p_i^*\} > E_{min}$. It follows that $E_{max} - \max_{i \in \mathcal{N}} \{(\tau^* - \tau_i^*)p_i^*\} > E_{min}$, or $\frac{E_{max} - E_{min}}{\max_{i \in \mathcal{N}} \{(\tau^* - \tau_i^*)p_i^*\}} > 1$. Thus

$$\gamma = \min_{i \in \mathcal{N}} \left\{ \frac{E_{max} - E_{min}}{(\tau^* - \tau_i^*)p_i^*} \right\} - 1 = \frac{E_{max} - E_{min}}{\max_{i \in \mathcal{N}} \{(\tau^* - \tau_i^*)p_i^*\}} - 1 > 0.$$

The feasibility of $\hat{\varphi}$ can be verified similarly as in the proof of Lemma 1.

We now show that this new feasible solution $\hat{\varphi}$ can offer a better (increased) objective value. By (4), we have $\frac{\hat{\tau}_{vac}}{\hat{\tau}} = 1 - \frac{\hat{\tau}_p}{\hat{\tau}} - \frac{\sum_{i \in \mathcal{N}} \hat{\tau}_i}{\hat{\tau}}$. Since $\hat{\tau} = (1 + \gamma)\tau^*$, $\hat{\tau}_i = (1 + \gamma)\tau_i^*$, $\hat{\tau}_p = \tau_p^*$, it follows that $\frac{\hat{\tau}_{vac}}{\hat{\tau}} = 1 - \frac{\tau_p^*}{(1 + \gamma)\tau^*} - \frac{\sum_{i \in \mathcal{N}} (1 + \gamma)\tau_i^*}{(1 + \gamma)\tau^*} > 1 - \frac{\tau_p^*}{\tau^*} - \frac{\sum_{i \in \mathcal{N}} \tau_i^*}{\tau^*} = \frac{\tau_{vac}^*}{\tau^*}$, i.e., $\frac{\hat{\tau}_{vac}}{\hat{\tau}} > \frac{\tau_{vac}^*}{\tau^*}$. This contradicts the assumption that φ^* is an optimal solution. ■

V. OPTIMAL TRAVELING PATH

In this section, we show that the WCV must move along the shortest Hamiltonian cycle in an optimal solution, which is formally stated in the following theorem.

Theorem 1: In an optimal solution with the maximum $\frac{\tau_{vac}}{\tau}$, the WCV must travel along the shortest Hamiltonian cycle that connects all the sensor nodes and the service station.

Proof: Theorem 1 can be proved by contradiction. That is, if there is an optimal solution $\varphi^* = (P^*, f_{ij}^*, f_{iB}^*, \tau^*, \tau_i^*, \tau_p^*, \tau_{vac}^*, p_i^*)$, where the WCV does not move along the shortest Hamiltonian cycle, then we can construct a new solution $\hat{\varphi} = (\hat{P}, \hat{f}_{ij}, \hat{f}_{iB}, \hat{\tau}, \hat{\tau}_i, \hat{\tau}_p, \hat{\tau}_{vac}, \hat{p}_i)$, with the WCV moving along the shortest Hamiltonian cycle and with an improved objective.

By assumption, P^* in φ^* does not follow the shortest Hamiltonian cycle. The new solution is constructed as follows. Let

\hat{P} follow the shortest Hamiltonian cycle (by either direction), $\hat{f}_{ij} = f_{ij}^*$, $\hat{f}_{iB} = f_{iB}^*$, $\hat{\tau} = \tau^*$, $\hat{\tau}_i = \tau_i^*$, $\hat{p}_i = p_i^*$, $\hat{\tau}_{\hat{P}}$ is the traveling time on path \hat{P} , and

$$\hat{\tau}_{\text{vac}} = \tau_{\text{vac}}^* + \tau_{P^*} - \hat{\tau}_{\hat{P}}. \quad (8)$$

Now, we show that the constructed solution $\hat{\varphi}$ is feasible. To verify feasibility, we need to show that $\hat{\varphi}$ satisfies flow conservation constraint (1), time constraint (4), and energy constraints (5) and (7). Since φ^* is a feasible solution, it satisfies (1), (4), (5), and (7). Since we have $\hat{f}_{ij} = f_{ij}^*$, $\hat{f}_{iB} = f_{iB}^*$, $\hat{\tau} = \tau^*$, $\hat{\tau}_i = \tau_i^*$, and $\hat{p}_i = p_i^*$ in $\hat{\varphi}$, the constraints (1), (5), and (7) also hold by $\hat{\varphi}$. To show that $\hat{\varphi}$ also satisfies (4), we have

$$\begin{aligned} \hat{\tau}_{\hat{P}} + \sum_{i \in \mathcal{N}} \hat{\tau}_i + \hat{\tau}_{\text{vac}} &= \hat{\tau}_{\hat{P}} + \sum_{i \in \mathcal{N}} \tau_i^* + (\tau_{\text{vac}}^* + \tau_{P^*} - \hat{\tau}_{\hat{P}}) \\ &= \sum_{i \in \mathcal{N}} \tau_i^* + \tau_{\text{vac}}^* + \tau_{P^*} = \tau^* = \hat{\tau} \end{aligned}$$

where the first equality follows from (8), the second equality follows by the feasibility of φ^* and (4), and the third equality follows by $\hat{\tau} = \tau^*$ during construction.

To show $\frac{\hat{\tau}_{\text{vac}}}{\hat{\tau}} > \frac{\tau_{\text{vac}}^*}{\tau^*}$, recall that \hat{P} follows the shortest Hamiltonian cycle, while P^* does not, i.e., the traveling distance $D_{P^*} > \hat{D}_{\hat{P}}$. Therefore, the traveling time $\tau_{P^*} > \hat{\tau}_{\hat{P}}$. Then, by (8), $\hat{\tau}_{\text{vac}} = \tau_{\text{vac}}^* + \tau_{P^*} - \hat{\tau}_{\hat{P}} > \tau_{\text{vac}}^*$, or $\frac{\hat{\tau}_{\text{vac}}}{\hat{\tau}} > \frac{\tau_{\text{vac}}^*}{\tau^*} = \frac{\tau_{\text{vac}}^*}{\tau^*}$. However, $\frac{\hat{\tau}_{\text{vac}}}{\hat{\tau}} > \frac{\tau_{\text{vac}}^*}{\tau^*}$ contradicts the assumption that φ^* is optimal. This completes the proof. ■

Theorem 1 says that the WCV should move along the shortest Hamiltonian cycle, which can be obtained by solving the well-known Traveling Salesman Problem (TSP) (see, e.g., [4] and [20]). Denote D_{TSP} as the traveling distance in the shortest Hamiltonian cycle, and let $\tau_{\text{TSP}} = D_{\text{TSP}}/V$. Then, with the optimal traveling path, (4) becomes

$$\tau_{\text{TSP}} + \tau_{\text{vac}} + \sum_{i \in \mathcal{N}} \tau_i = \tau \quad (9)$$

and the solution for a renewable cycle becomes $\varphi = (P_{\text{TSP}}, f_{ij}, f_{iB}, \tau, \tau_i, \tau_{\text{TSP}}, \tau_{\text{vac}}, p_i)$. Since the optimal traveling path is determined, the solution can be simplified as $\varphi = (f_{ij}, f_{iB}, \tau, \tau_i, \tau_{\text{vac}}, p_i)$.

We note that the shortest Hamiltonian cycle may not be unique. Since any shortest Hamiltonian cycle has the same total path distance and traveling time τ_{TSP} , the selection of a particular shortest Hamiltonian cycle does not affect constraint (9) and yields the same optimal objective. This insight is formally stated in the following corollary.

Corollary 1.1: Any shortest Hamiltonian cycle achieves the same optimal objective.

We also note that to travel the shortest Hamiltonian cycle, there are two (opposite) outgoing directions for the WCV to start from its home service station. Since the proof of Theorem 1 is independent of the starting direction for the WCV, either direction will yield an optimal solution with the same objective value, although some variables in each optimal solution will have different values. We have the following corollary.

Corollary 1.2: The WCV can follow either direction to traverse the shortest Hamiltonian cycle, both of which will achieve the same optimal objective. There exist two optimal solutions corresponding to the two opposite directions, with

identical values of $f_{ij}, f_{iB}, \tau, \tau_i, \tau_{\text{TSP}}, \tau_{\text{vac}}, p_i$, but different values of a_i [by (3)] and E_i [by (6)] due to the difference in their respective renewable cycles, where $i, j \in \mathcal{N}, i \neq j$.

VI. PROBLEM FORMULATION AND SOLUTION

A. Mathematical Formulation

Summarizing the objective and all the constraints in Sections III–V, our problem can be formulated as follows:

OPT

$$\begin{aligned} \max \quad & \frac{\tau_{\text{vac}}}{\tau} \\ \text{s.t.} \quad & \sum_{j \in \mathcal{N}} f_{ij} + f_{iB} - \sum_{k \in \mathcal{N}} f_{ki} = R_i \quad (i \in \mathcal{N}) \\ & \rho \cdot \sum_{k \in \mathcal{N}} f_{ki} + \sum_{j \in \mathcal{N}} C_{ij} \cdot f_{ij} \\ & \quad + C_{iB} \cdot f_{iB} - p_i = 0 \quad (i \in \mathcal{N}) \quad (10) \\ & \tau - \sum_{i \in \mathcal{N}} \tau_i - \tau_{\text{vac}} = \tau_{\text{TSP}} \quad (11) \\ & \tau \cdot p_i - U \cdot \tau_i = 0 \quad (i \in \mathcal{N}) \quad (12) \\ & (\tau - \tau_i) \cdot p_i \leq E_{\max} - E_{\min} \quad (i \in \mathcal{N}) \quad (13) \end{aligned}$$

$$f_{ij}, f_{iB}, \tau_i, \tau, \tau_{\text{vac}}, p_i \geq 0 \quad (i, j \in \mathcal{N}, i \neq j).$$

In this problem, flow rates f_{ij} and f_{iB} , time intervals τ, τ_i , and τ_{vac} , and power consumption p_i are optimization variables, and $R_i, \rho, C_{ij}, C_{iB}, U, E_{\max}, E_{\min}$, and τ_{TSP} are constants. This problem has both nonlinear objective ($\frac{\tau_{\text{vac}}}{\tau}$) and nonlinear terms (τp_i and $\tau_i p_i$) in constraints (12) and (13).

Note that there are two possible outcomes for optimization problem OPT: Either an optimal solution exists, or OPT is infeasible. There are several scenarios where the latter outcome may occur, e.g.: 1) the energy charging rate of WCV is too small or the energy consumption rate of a node is too large; 2) the time interval between WCV's visits at any node is too large. As a result, some constraints in Problem OPT will not hold. These are physical limitations for a WCV to achieve a renewable network lifetime for a WSN.

We note that in the above formulation, only constant τ_{TSP} is related to the shortest Hamiltonian cycle. Since this value does not depend on the traveling direction along the Hamiltonian cycle, an optimal solution to Problem OPT will work for either direction and yields different renewable cycle for each direction.

B. Reformulation

We first use a change-of-variable technique to simplify the formulation. For the nonlinear objective $\frac{\tau_{\text{vac}}}{\tau}$, we define

$$\eta_{\text{vac}} = \frac{\tau_{\text{vac}}}{\tau}. \quad (14)$$

For (11), we divide both sides by τ and get $\tau_{\text{TSP}} \cdot \frac{1}{\tau} + \eta_{\text{vac}} + \sum_{i \in \mathcal{N}} \frac{\tau_i}{\tau} = 1$. To remove the nonlinear terms $\frac{1}{\tau}$ and $\frac{\tau_i}{\tau}$ in the above equation, we define

$$\eta_i = \frac{\tau_i}{\tau} \quad (i \in \mathcal{N}) \quad (15)$$

$$h = \frac{1}{\tau}. \quad (16)$$

Then, (11) is reformulated as $\tau_{\text{TSP}} \cdot h + \eta_{\text{vac}} + \sum_{i \in \mathcal{N}} \eta_i = 1$, or equivalently

$$h = \frac{1 - \sum_{i \in \mathcal{N}} \eta_i - \eta_{\text{vac}}}{\tau_{\text{TSP}}}. \quad (17)$$

Similarly, (12) and (13) can be reformulated (by dividing both sides by τ) as

$$p_i = U \cdot \eta_i \quad (i \in \mathcal{N}) \quad (18)$$

$$(1 - \eta_i) \cdot p_i \leq (E_{\text{max}} - E_{\text{min}}) \cdot h \quad (i \in \mathcal{N}). \quad (19)$$

By (17) and (18), constraint (19) can be rewritten as $(1 - \eta_i) \cdot$

$$U \eta_i \leq (E_{\text{max}} - E_{\text{min}}) \frac{1 - \sum_{k \in \mathcal{N}} \eta_k - \eta_{\text{vac}}}{\tau_{\text{TSP}}}, \text{ or}$$

$$\eta_{\text{vac}} \leq 1 - \sum_{k \in \mathcal{N}} \eta_k - \frac{U \cdot \tau_{\text{TSP}}}{E_{\text{max}} - E_{\text{min}}} \cdot \eta_i \cdot (1 - \eta_i) \quad (i \in \mathcal{N}).$$

By (18), constraint (10) can be rewritten as

$$\rho \cdot \sum_{k \in \mathcal{N}} f_{ki} + \sum_{j \in \mathcal{N}} C_{ij} f_{ij} + C_{iB} f_{iB} - U \eta_i = 0 \quad (i \in \mathcal{N}).$$

Hence, the problem OPT is reformulated as follows:

OPT-R

max η_{vac}

$$\text{s.t. } \sum_{j \in \mathcal{N}} f_{ij} + f_{iB} - \sum_{k \in \mathcal{N}} f_{ki} = R_i \quad (i \in \mathcal{N})$$

$$\rho \cdot \sum_{k \in \mathcal{N}} f_{ki} + \sum_{j \in \mathcal{N}} C_{ij} f_{ij} + C_{iB} f_{iB} - U \eta_i = 0 \quad (i \in \mathcal{N}) \quad (20)$$

$$\eta_{\text{vac}} \leq 1 - \sum_{k \in \mathcal{N}} \eta_k - \frac{U \cdot \tau_{\text{TSP}}}{E_{\text{max}} - E_{\text{min}}} \cdot \eta_i \cdot (1 - \eta_i) \quad (i \in \mathcal{N}) \quad (21)$$

$$f_{ij}, f_{iB} \geq 0, 0 \leq \eta_i, \eta_{\text{vac}} \leq 1 \quad (i, j \in \mathcal{N}, i \neq j).$$

In this problem, f_{ij} , f_{iB} , η_i , and η_{vac} are optimization variables, and R_i , ρ , C_{ij} , C_{iB} , U , E_{max} , E_{min} , and τ_{TSP} are constants. The following algorithm shows how to obtain a solution to Problem OPT once we obtain a solution to Problem OPT-R.

Algorithm 1: Once we solve Problem OPT-R, we can obtain a corresponding solution to Problem OPT (i.e., calculate the values for τ , τ_i , τ_{vac} , and p_i) as follows: h by (17), τ by (16), τ_i by (15), τ_{vac} by (14), and p_i by (18).

After reformulation, the objective function and the constraints become linear except (21), where we have a second-order η_i^2 term, with $0 \leq \eta_i \leq 1$. In the next section, we present an efficient technique to approximate this second-order nonlinear term (with performance guarantee). Subsequently, we develop an efficient near-optimal solution to our optimization problem.

Remark 1: In our optimization problem, data routing and charging time are closely coupled. One may want to decouple routing from the charging problem and require certain energy-efficient routing, e.g., the minimum-energy routing.³ How-

³Here, minimum-energy routing refers to using the least-energy route to transport data from its source to destination.

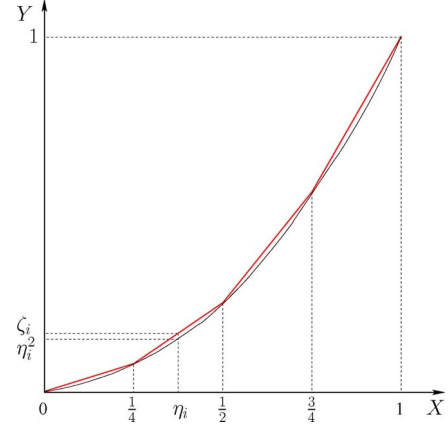


Fig. 4. Illustration of piecewise linear approximation (with $m = 4$) for the curve (η_i, η_i^2) , $0 \leq \eta_i \leq 1$.

ever, minimum-energy routing cannot guarantee optimality. This is because, to maximize η_{vac} , by (21), we need to minimize $\max_{i \in \mathcal{N}} \left\{ \sum_{k \in \mathcal{N}} \eta_k + \frac{U \cdot \tau_{\text{TSP}}}{E_{\text{max}} - E_{\text{min}}} \cdot \eta_i \cdot (1 - \eta_i) \right\}$, i.e., minimize $\left\{ \sum_{k \in \mathcal{N}} \eta_k + \max_{i \in \mathcal{N}} \left\{ \frac{U \cdot \tau_{\text{TSP}}}{E_{\text{max}} - E_{\text{min}}} \cdot \eta_i \cdot (1 - \eta_i) \right\} \right\}$. However, under minimum-energy routing, we can only guarantee that $\sum_{i \in \mathcal{N}} \left(\rho \cdot \sum_{k \in \mathcal{N}} f_{ki} + \sum_{j \in \mathcal{N}} C_{ij} f_{ij} + C_{iB} f_{iB} \right)$ is minimized. By the relationship in (20), minimizing $\sum_{i \in \mathcal{N}} \left(\rho \cdot \sum_{k \in \mathcal{N}} f_{ki} + \sum_{j \in \mathcal{N}} C_{ij} f_{ij} + C_{iB} f_{iB} \right)$ is equivalent to minimizing $\sum_{i \in \mathcal{N}} \eta_i$, which is only part of $\sum_{k \in \mathcal{N}} \eta_k + \max_{i \in \mathcal{N}} \left\{ \frac{U \cdot \tau_{\text{TSP}}}{E_{\text{max}} - E_{\text{min}}} \cdot \eta_i \cdot (1 - \eta_i) \right\}$. Therefore, minimum-energy routing cannot guarantee the optimality of our problem. This insight will be confirmed by our numerical results in Section VIII.

C. Near-Optimal Solution

Roadmap: Our roadmap to solve Problem OPT is as follows. First, we employ a piecewise linear approximation for the quadratic terms (η_i^2) in Problem OPT-R. This approximation relaxes the corresponding nonlinear constraints into linear constraints, which allows for the problem to be solved by a solver such as CPLEX [11]. Based on the solution from CPLEX, we construct a feasible solution to Problem OPT. In Section VI-D, we prove the near-optimality of this feasible solution.

Piecewise Linear Approximation for η_i^2 : Note that the only nonlinear terms in the formulation are η_i^2 , $i \in \mathcal{N}$. Furthermore, η_i lies in the interval $[0, 1]$, which is small. This motivates us to employ a piecewise linear approximation for the quadratic terms η_i^2 .

The key idea is to use m piecewise linear segments to approximate the quadratic curve (see Fig. 4). That is, for curve (η_i, η_i^2) , $0 \leq \eta_i \leq 1$, we construct a piecewise linear approximation (η_i, ζ_i) by connecting points $\left(\frac{k}{m}, \frac{k^2}{m^2} \right)$, $k = 0, 1, \dots, m$. The setting of m will determine the level of accuracy and will be studied in Section VI-D.

We now represent the piecewise linear curve (η_i, ζ_i) for $0 \leq \eta_i \leq 1$ mathematically. For $k = 0, 1, \dots, m$, any point (η_i, ζ_i) on the piecewise linear curve within the k th segment (i.e., lying

within two endpoints $\left(\frac{k-1}{m}, \frac{(k-1)^2}{m^2}\right)$ and $\left(\frac{k}{m}, \frac{k^2}{m^2}\right)$ can be represented by

$$\eta_i = \lambda_{i,k-1} \cdot \frac{k-1}{m} + \lambda_{i,k} \cdot \frac{k}{m} \quad (22)$$

$$\zeta_i = \lambda_{i,k-1} \cdot \frac{(k-1)^2}{m^2} + \lambda_{i,k} \cdot \frac{k^2}{m^2} \quad (23)$$

where $\lambda_{i,k-1}$ and $\lambda_{i,k}$ are two weights and satisfy the following constraints:

$$\lambda_{i,k-1} + \lambda_{i,k} = 1 \quad (24)$$

$$0 \leq \lambda_{i,k-1}, \lambda_{i,k} \leq 1. \quad (25)$$

Since $y = x^2$ is a convex function, the piecewise linear approximation curve (η_i, ζ_i) lies above the curve (η_i, η_i^2) , $0 \leq \eta_i \leq 1$. Thus, we have $\zeta_i \geq \eta_i^2$ (see Fig. 4). The following lemma characterizes the approximation error $\zeta_i - \eta_i^2$ as a function of m .

Lemma 3: $\zeta_i - \eta_i^2 \leq \frac{1}{4m^2}$ for $i \in \mathcal{N}$.

The proof of this lemma is straightforward and is given in [27].

Note that the mathematical representation in (22)–(25) is for a given k th segment, $k = 1, 2, \dots, m$. We now give a mathematical formulation for the entire piecewise linear curve. Denote z_{ik} , $1 \leq k \leq m$, a binary variable indicating whether η_i falls within the k th segment, i.e., if $\frac{k-1}{m} \leq \eta_i < \frac{k}{m}$, then $z_{ik} = 1$, otherwise, $z_{ik} = 0$. Since η_i can only fall in one of the m segments, we have

$$\sum_{k=1}^m z_{ik} = 1. \quad (26)$$

With the definition of z_{ik} , $1 \leq k \leq m$, we can formulate (22)–(24) for the entire piecewise linear curve. First, we show how λ_{ik} relates to z_{ik} , $1 \leq k \leq m$. Based on (22)–(24), when η_i falls within the k th segment, we can only have $\lambda_{i,k-1}$ and $\lambda_{i,k}$ positive while all other $\lambda_{i,j}$ ($j \neq k-1, k$) must be zero. That is, $\lambda_{i0} > 0$ only if $z_{i1} = 1$; $\lambda_{ik} > 0$ only if $z_{ik} = 1$ or $z_{i,k+1} = 1$, $1 \leq k < m$; and $\lambda_{im} > 0$ only if $z_{im} = 1$. These relationships can be written as follows:

$$\lambda_{i0} \leq z_{i1} \quad (27)$$

$$\lambda_{ik} \leq z_{ik} + z_{i,k+1} \quad (1 \leq k < m) \quad (28)$$

$$\lambda_{im} \leq z_{im}. \quad (29)$$

The above three constraints ensure that there are at most two adjacent positive λ values for each η_i . Equations (22)–(24) can now be rewritten for the entire piecewise linear curve as follows:

$$\eta_i = \sum_{k=0}^m \lambda_{ik} \cdot \frac{k}{m} \quad (30)$$

$$\zeta_i = \sum_{k=0}^m \lambda_{ik} \cdot \frac{k^2}{m^2} \quad (31)$$

$$\sum_{k=0}^m \lambda_{ik} = 1. \quad (32)$$

Relaxed Linear Formulation: By replacing η_i^2 with ζ_i in (21), we have

$$\eta_{\text{vac}} \leq 1 - \sum_{k \in \mathcal{N}} \eta_k - \frac{U \tau_{\text{TSP}}}{E_{\text{max}} - E_{\text{min}}} (\eta_i - \zeta_i) \quad (i \in \mathcal{N}). \quad (33)$$

By adding the new constraints (26)–(32) to the model, we obtain the following linear relaxed formulation:

OPT-L

$$\begin{aligned} \max \quad & \eta_{\text{vac}} \\ \text{s.t.} \quad & \sum_{j \in \mathcal{N}} f_{ij} + f_{iB} - \sum_{k \in \mathcal{N}} f_{ki} = R_i \quad (i \in \mathcal{N}) \\ & \rho \cdot \sum_{k \in \mathcal{N}} f_{ki} + \sum_{j \in \mathcal{N}} C_{ij} \cdot f_{ij} + C_{iB} \cdot f_{iB} - U \cdot \eta_i \\ & \quad = 0 \quad (i \in \mathcal{N}) \\ & \eta_{\text{vac}} \leq 1 - \sum_{k \in \mathcal{N}} \eta_k - \frac{U \tau_{\text{TSP}}}{E_{\text{max}} - E_{\text{min}}} \\ & \quad \cdot (\eta_i - \zeta_i) \quad (i \in \mathcal{N}) \\ & \sum_{k=1}^m z_{ik} = 1 \quad (i \in \mathcal{N}) \\ & \lambda_{i0} - z_{i1} \leq 0 \quad (i \in \mathcal{N}) \\ & \lambda_{ik} - z_{ik} - z_{i,k+1} \leq 0 \quad (i \in \mathcal{N}, 1 \leq k < m) \\ & \lambda_{im} - z_{im} \leq 0 \quad (i \in \mathcal{N}) \\ & \eta_i - \sum_{k=0}^m \frac{k}{m} \cdot \lambda_{ik} = 0 \quad (i \in \mathcal{N}) \\ & \zeta_i - \sum_{k=0}^m \frac{k^2}{m^2} \cdot \lambda_{ik} = 0 \quad (i \in \mathcal{N}) \\ & \sum_{k=0}^m \lambda_{ik} = 1 \quad (i \in \mathcal{N}) \\ & f_{ij}, f_{iB} \geq 0, 0 \leq \eta_i, \eta_{\text{vac}}, \zeta_i \leq 1 \quad (i, j \in \mathcal{N}, i \neq j) \\ & z_{ik} \in \{0, 1\} \quad (i \in \mathcal{N}, 1 \leq k \leq m) \\ & 0 \leq \lambda_{ik} \leq 1 \quad (i \in \mathcal{N}, 0 \leq k \leq m) \end{aligned}$$

where f_{ij} , f_{iB} , η_i , η_{vac} , z_{ik} , λ_{ik} , and ζ_i are variables, and R_i , ρ , C_{ij} , C_{iB} , U , E_{max} , E_{min} , and τ_{TSP} are constants. This new formulation can be solved by a solver such as CPLEX [11].

Construction of a Feasible Near-Optimal Solution: The solution to Problem OPT-L is likely to be infeasible to Problem OPT-R (and Problem OPT). However, based on this solution, we can construct a feasible solution to Problem OPT.

Suppose that $\hat{\psi} = (\hat{f}_{ij}, \hat{f}_{iB}, \hat{\eta}_i, \hat{\eta}_{\text{vac}}, \hat{z}_{ik}, \hat{\lambda}_{ik}, \hat{\zeta}_i)$ is the solution obtained for Problem OPT-L. By observing $(\hat{f}_{ij}, \hat{f}_{iB}, \hat{\eta}_i, \hat{\eta}_{\text{vac}})$, we find that it satisfies all constraints to Problem OPT-R except (21). To construct a feasible solution $\psi = (f_{ij}, f_{iB}, \eta_i, \eta_{\text{vac}})$ to Problem OPT-R, we let $f_{ij} = \hat{f}_{ij}$, $f_{iB} = \hat{f}_{iB}$, $\eta_i = \hat{\eta}_i$. For η_{vac} , in order to satisfy (21), we define

$$\eta_{\text{vac}} = \min_{i \in \mathcal{N}} \left\{ 1 - \sum_{k \in \mathcal{N}} \hat{\eta}_k - \frac{U \cdot \tau_{\text{TSP}}}{E_{\text{max}} - E_{\text{min}}} \hat{\eta}_i (1 - \hat{\eta}_i) \right\}.$$

It is easy to verify that this newly constructed solution ψ satisfies all the constraints for Problem OPT-R. Once we have this solution to Problem OPT-R, we can easily find a solution to Problem OPT via Algorithm 1.

D. Proof of Near-Optimality

In this section, we quantify the performance gap between the optimal objective (unknown, denoted by η_{vac}^*) and the objective (denoted by η_{vac}) obtained by the feasible solution ψ that we derived in the last section. Naturally, we expect such a performance gap to be a function of m , i.e., the number of segments that we use in the piecewise linear approximation. This result will be stated in Lemma 4. Based on this result, we can obtain an important inverse result (in Theorem 2), which shows how to set m such that $\eta_{vac}^* - \eta_{vac} \leq \epsilon$ for a given target performance gap ϵ ($0 < \epsilon \ll 1$).

Lemma 4: For the feasible solution ψ with objective value η_{vac} , we have $\eta_{vac}^* - \eta_{vac} \leq \frac{U \cdot \tau_{TSP}}{4(E_{max} - E_{min})} \cdot \frac{1}{m^2}$.

Proof: Denote $\hat{\eta}_{vac}$ as the objective value obtained by the solution ψ to the relaxed linear problem OPT-L. Since Problem OPT-L is a relaxation of Problem OPT-R, $\hat{\eta}_{vac}$ is an upper bound of η_{vac}^* , i.e., $\eta_{vac}^* \leq \hat{\eta}_{vac}$. Therefore

$$\begin{aligned} \eta_{vac}^* - \eta_{vac} &\leq \hat{\eta}_{vac} - \eta_{vac} \\ &= \left[1 - \sum_{k \in \mathcal{N}} \hat{\eta}_k - \frac{U \tau_{TSP}}{E_{max} - E_{min}} \cdot (\eta_{max} - \zeta_{max}) \right] \\ &\quad - \left[1 - \sum_{k \in \mathcal{N}} \hat{\eta}_k - \frac{U \tau_{TSP}}{E_{max} - E_{min}} \cdot \eta_{max} \cdot (1 - \eta_{max}) \right] \\ &= \frac{U \tau_{TSP}}{E_{max} - E_{min}} (\zeta_{max} - \eta_{max}^2) \leq \frac{U \tau_{TSP}}{4(E_{max} - E_{min})} \cdot \frac{1}{m^2} \end{aligned}$$

where the second equality holds by [27, Lemmas 5 and 6] (omitted here to conserve space), and the fourth inequality holds by Lemma 3. ■

Based on Lemma 4, the following theorem shows how to set m such that $\eta_{vac}^* - \eta_{vac} \leq \epsilon$ for a given target performance gap ϵ ($0 < \epsilon \ll 1$).

Theorem 2: For a given ϵ , $0 < \epsilon \ll 1$, if $m = \left\lceil \sqrt{\frac{U \tau_{TSP}}{4\epsilon(E_{max} - E_{min})}} \right\rceil$, then we have $\eta_{vac}^* - \eta_{vac} \leq \epsilon$.

Proof: Lemma 4 shows that the performance gap is $\eta_{vac}^* - \eta_{vac} \leq \frac{U \tau_{TSP}}{4(E_{max} - E_{min})} \cdot \frac{1}{m^2}$. Therefore, if we set

$$\begin{aligned} m &= \left\lceil \sqrt{\frac{U \tau_{TSP}}{4\epsilon(E_{max} - E_{min})}} \right\rceil \geq \sqrt{\frac{U \tau_{TSP}}{4\epsilon(E_{max} - E_{min})}}, \text{ then we have} \\ \eta_{vac}^* - \eta_{vac} &\leq \frac{U \tau_{TSP}}{4(E_{max} - E_{min})} \cdot \frac{1}{m^2} \\ &\leq \frac{U \tau_{TSP}}{4(E_{max} - E_{min})} \cdot \frac{4\epsilon(E_{max} - E_{min})}{U \tau_{TSP}} = \epsilon. \end{aligned}$$

This completes the proof. ■

With Theorem 2, we display the complete solution procedure on how to obtain a near-optimal solution to Problem OPT in Fig. 5.

VII. CONSTRUCTING AN INITIAL TRANSIENT CYCLE

In Section IV, we skipped discussion on how to construct an initial transient cycle before the first renewable cycle. Now with the optimal traveling path P (the shortest Hamiltonian cycle)

Construction of a Near-Optimal Solution

1. Given a target performance gap ϵ .
2. Let $m = \left\lceil \sqrt{\frac{U \tau_{TSP}}{4\epsilon(E_{max} - E_{min})}} \right\rceil$.
3. Solve Problem OPT-L with m segments by CPLEX, and obtain its solution $\hat{\psi} = (\hat{f}_{ij}, \hat{f}_{iB}, \hat{\eta}_i, \hat{\lambda}_{ik}, \hat{\zeta}_i)$.
4. Construct a feasible solution $\psi = (f_{ij}, f_{iB}, \eta_i, \eta_{vac})$ for Problem OPT-R by letting $f_{ij} = \hat{f}_{ij}$, $f_{iB} = \hat{f}_{iB}$, $\eta_i = \hat{\eta}_i$ and $\eta_{vac} = \min_{i \in \mathcal{N}} \{1 - \sum_{k \in \mathcal{N}} \hat{\eta}_k - \frac{U \tau_{TSP}}{E_{max} - E_{min}} \cdot \hat{\eta}_i \cdot (1 - \hat{\eta}_i)\}$.
5. Obtain a near-optimal solution $(f_{ij}, f_{iB}, \tau, \tau_i, \tau_{vac}, p_i)$ to Problem OPT by Algorithm 1.

Fig. 5. Summary of how to construct a near-optimal solution.

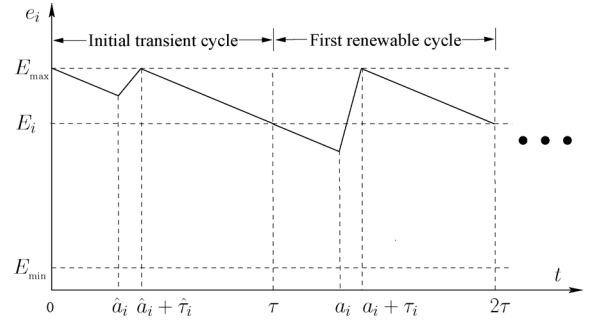


Fig. 6. Illustration of energy behavior for the initial transient cycle and how it connects to the first renewable cycle.

and the feasible near-optimal solution $(f_{ij}, f_{iB}, \tau, \tau_i, \tau_{vac}, p_i)$ obtained in Section VI, we are ready to construct an initial transient cycle.

Unlike a renewable energy cycle at node i , which starts and ends with the same energy level E_i , the initial transient starts with E_{max} and ends with E_i . Specifically, the initial transient cycle must meet the following criterion.

Criterion 1: At each node $i \in \mathcal{N}$, its initial transient cycle must meet the following criteria: (i) $e_i(0) = E_{max}$ and $e_i(\tau) = E_i$; and (ii) $e_i(t) \geq E_{min}$ for $t \in [0, \tau]$.

We now construct an initial cycle to meet the above criterion. First, we need to calculate E_i , $i \in \mathcal{N}$. From (6), we have $E_i = E_{max} - (2\tau - a_i - \tau_i)p_i$, where a_i can be obtained by (3).

For a solution $\varphi = (P, f_{ij}, f_{iB}, \tau, \tau_i, \tau_p, \tau_{vac}, p_i, U)$ corresponding to a renewable energy cycle for $t \geq \tau$, we construct $\hat{\varphi} = (\hat{P}, \hat{f}_{ij}, \hat{f}_{iB}, \hat{\tau}, \hat{\tau}_i, \hat{\tau}_p, \hat{\tau}_{vac}, \hat{p}_i, u_i)$ for the initial transient cycle for $t \in [0, \tau]$ by letting $\hat{P} = P$, $\hat{f}_{ij} = f_{ij}$, $\hat{f}_{iB} = f_{iB}$, $\hat{\tau} = \tau$, $\hat{\tau}_i = \tau_i$, $\hat{\tau}_p = \tau_p$, $\hat{\tau}_{vac} = \tau_{vac}$, $\hat{p}_i = p_i$ and

$$u_i = \frac{p_i \hat{a}_i}{\tau_i} + p_i \quad (34)$$

where u_i is the charging rate at node i during the initial transient cycle and \hat{a}_i is the arrival time of the WCV at node i in the initial transient cycle (see Fig. 6).

We now need to show that $u_i \leq U$, where U is the full charging rate. First, we have

$$\begin{aligned} \hat{a}_{\pi_i} &= \sum_{k=0}^{i-1} \frac{\hat{D}_{\pi_k \pi_{k+1}}}{V} + \sum_{k=1}^{i-1} \hat{\tau}_{\pi_k} \\ &= \sum_{k=0}^{i-1} \frac{D_{\pi_k \pi_{k+1}}}{V} + \sum_{k=1}^{i-1} \tau_{\pi_k} = a_{\pi_i} - \tau \end{aligned} \quad (35)$$

where the second equality holds by $\hat{P} = P$ and $\hat{\tau}_i = \tau_i$, and the last equality follows from (3). Furthermore, by (5), we have $U \cdot \tau_i = \tau \cdot p_i = (2\tau - \tau) \cdot p_i \geq (a_i + \tau_i - \tau) \cdot p_i$. It follows that

$$(a_i - \tau) \cdot p_i \leq (U - p_i) \cdot \tau_i. \quad (36)$$

Then, we have

$$u_i = \frac{p_i \hat{a}_i}{\tau_i} + p_i = \frac{p_i(a_i - \tau)}{\tau_i} + p_i \leq \frac{(U - p_i) \cdot \tau_i}{\tau_i} + p_i = U$$

where the first equality follows from (34), the second equality follows from (35), and the third inequality follows from (36).

For the newly constructed $\hat{\varphi}$, we have the following theorem.

Theorem 3: The constructed $\hat{\varphi}$ is a feasible transient cycle.

Proof: To prove that $\hat{\varphi}$ is a feasible initial transient cycle, we need to show that the newly constructed $\hat{\varphi}$ satisfies Criterion 1. By our assumption, $e_i(0) = E_{\max}$. At time $(\hat{a}_i + \hat{\tau}_i)$, we have

$$\begin{aligned} e_i(\hat{a}_i + \hat{\tau}_i) &= e_i(0) - \hat{p}_i \cdot \hat{a}_i + (u_i - \hat{p}_i) \cdot \hat{\tau}_i \\ &= E_{\max} - p_i \cdot (a_i - \tau) + (u_i - p_i) \cdot \tau_i \\ &= E_{\max} - p_i \cdot (a_i - \tau + \tau_i) + u_i \cdot \tau_i = E_{\max} \end{aligned} \quad (37)$$

where the second equality follows since $e_i(0) = E_{\max}$, $\hat{p}_i = p_i$, $\hat{a}_i = a_i - \tau$, and $\hat{\tau}_i = \tau_i$, the last equality follows from (34) and (35). Therefore, the battery at node i is full when the WCV leaves it at $(\hat{a}_i + \hat{\tau}_i)$. At time τ , we have

$$\begin{aligned} e_i(\tau) &= e_i(\hat{a}_i + \hat{\tau}_i) - \hat{p}_i \cdot (\tau - (\hat{a}_i + \hat{\tau}_i)) \\ &= E_{\max} - p_i \cdot [\tau - (a_i - \tau + \tau_i)] \\ &= E_{\max} - p_i \cdot [2\tau - (a_i + \tau_i)] = e_i(2\tau) = E_i \end{aligned} \quad (38)$$

where the second equality follows from (37), and the fourth equality follows from (6). Therefore, Criterion 1(i) is met.

To show $e_i(t) \geq E_{\min}$ for $t \in [0, \tau]$, it is sufficient to show that $e_i(\hat{a}_i) \geq E_{\min}$ and $e_i(\tau) \geq E_{\min}$ since these two time instances are the local minimum for $e_i(t)$ during $t \in [0, \tau]$. We have

$$\begin{aligned} e_i(\hat{a}_i) &= e_i(0) - \hat{p}_i \cdot \hat{a}_i = E_{\max} - p_i \cdot (a_i - \tau) \\ &\geq E_i - p_i \cdot (a_i - \tau) = e_i(a_i) \geq E_{\min}. \end{aligned}$$

Also, by (38), $e_i(\tau) = E_i \geq E_{\min}$. Hence, $e_i(t) \geq E_{\min}$, for $t \in [0, \tau]$.

In summary, $\hat{\varphi}$ meets all the criteria of a feasible initial transient cycle. This completes the proof. ■

VIII. NUMERICAL RESULTS

In this section, we present some numerical results to demonstrate how our solution can produce a renewable WSN and some interesting properties with such a network.

A. Simulation Settings

We consider two randomly generated WSNs consisting of 50 and 100 nodes, respectively. The sensor nodes are deployed over a square area of 1×1 km². The data rate (i.e., R_i , $i \in \mathcal{N}$) from each node is randomly generated within $[1, 10]$ kb/s. The power consumption coefficients are $\beta_1 = 50$ nJ/b, $\beta_2 =$

TABLE I
LOCATION AND DATA RATE R_i FOR EACH NODE IN A 50-NODE NETWORK

Node Index	Location (m)	R_i (kb/s)	Node Index	Location (m)	R_i (kb/s)
1	(815, 276)	1	26	(758, 350)	9
2	(906, 680)	8	27	(743, 197)	1
3	(127, 655)	4	28	(392, 251)	4
4	(913, 163)	6	29	(655, 616)	4
5	(632, 119)	3	30	(171, 473)	9
6	(98, 498)	7	31	(706, 352)	5
7	(278, 960)	3	32	(32, 831)	10
8	(547, 340)	7	33	(277, 585)	1
9	(958, 585)	6	34	(46, 550)	3
10	(965, 224)	8	35	(97, 917)	2
11	(158, 751)	5	36	(823, 286)	2
12	(971, 255)	1	37	(695, 757)	8
13	(957, 506)	4	38	(317, 754)	6
14	(485, 699)	10	39	(950, 380)	6
15	(800, 891)	2	40	(34, 568)	2
16	(142, 959)	9	41	(439, 76)	8
17	(422, 547)	5	42	(382, 54)	7
18	(916, 139)	10	43	(766, 531)	4
19	(792, 149)	1	44	(795, 779)	6
20	(959, 258)	5	45	(187, 934)	6
21	(656, 841)	3	46	(490, 130)	1
22	(36, 254)	10	47	(446, 569)	3
23	(849, 814)	1	48	(646, 469)	2
24	(934, 244)	8	49	(709, 12)	2
25	(679, 929)	8	50	(755, 337)	3

0.0013 pJ/(b · m⁴), $\alpha = 4$, and $\rho = 50$ nJ/b [9]. The base station is assumed to be located at (500, 500) (in meters), and the home service station for the WCV is assumed to be at the origin. The traveling speed of the WCV is $V = 5$ m/s.

For the battery at a sensor node, we choose a regular NiMH battery, and its nominal cell voltage and the quantity of electricity is 1.2 V/2.5 Ah. We have $E_{\max} = 1.2$ V \times 2.5 A \times 3600 s = 10.8 kJ [19]. We let $E_{\min} = 0.05 \cdot E_{\max} = 540$ J. We assume the wireless energy transfer rate $U = 5$ W, which is well within feasible range [15].

We set the target $\epsilon = 0.01$ for the numerical results, i.e., our solution has an error no more than 0.01. The experiments were conducted on a DELL Precision T5400 with Intel Xeon 3.0 GHz and 16 GB RAM. All the network instances (with up to 100 nodes) were solved in seconds.

B. Results

50-Node Network: We first present complete results for the 50-node network. Table I gives the location of each node and its data rate for a 50-node network. The shortest Hamiltonian cycle is found by using the Concorde solver [4] and is shown in Fig. 7. For this optimal cycle, $D_{\text{TSP}} = 5821$ m and $\tau_{\text{TSP}} = 1164.2$ s. For the target $\epsilon = 0.01$, by Theorem 2, we have

$$\begin{aligned} m &= \left\lceil \sqrt{\frac{U \cdot \tau_{\text{TSP}}}{4\epsilon(E_{\max} - E_{\min})}} \right\rceil \\ &= \left\lceil \sqrt{\frac{5 \times 1164.2}{4 \times 0.01 \times (10800 - 540)}} \right\rceil = 4 \end{aligned}$$

which is a small number. In our solution, the cycle time $\tau = 30.73$ h, the vacation time $\tau_{\text{vac}} = 26.82$ h, and the objective $\eta_{\text{vac}} = 87.27\%$.

By Corollary 1.2, the WCV can follow either direction of the shortest Hamiltonian cycle while achieving the same objective

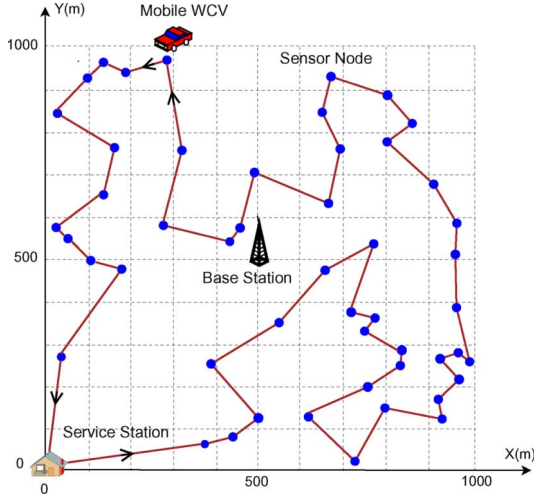


Fig. 7. Optimal traveling path for the WCV for the 50-node sensor network, assuming counter-clockwise traveling direction.

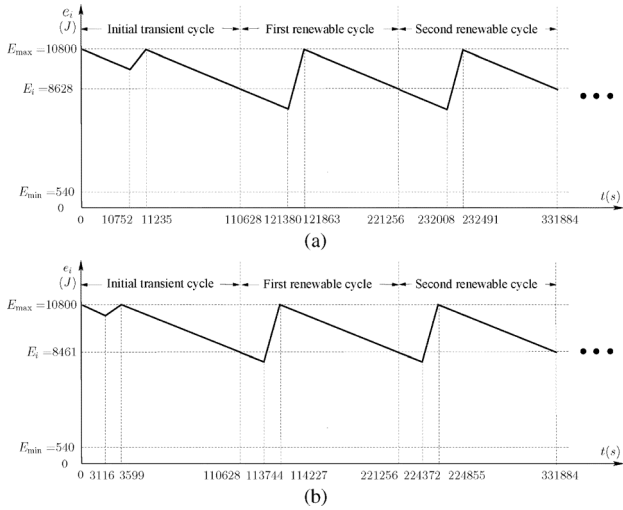


Fig. 8. Energy behavior of a sensor node (the 32nd) in the 50-node network during the initial transient cycle and the first two renewable cycles. (a) Traveling direction is counter-clockwise. (b) Traveling direction is clockwise.

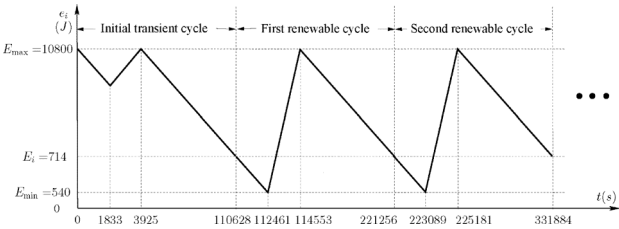


Fig. 9. Energy behavior of the bottleneck node (48th node) in the 50-node network. Traveling direction is counter-clockwise.

value $\eta_{vac} = 87.27\%$. Comparing the two solutions, the values for f_{ij} , f_{iB} , τ_i , τ_i , τ_{TSP} , τ_{vac} are identical, while the values of a_i and E_i are different. This observation can be verified by our simulation results in Table II (counterclockwise direction) and Table III (clockwise direction). As an example, Fig. 8(a) and (b) shows the energy cycle behavior of a sensor node (the 32nd node) under the two opposite traveling directions, respectively.

TABLE II
CASE OF COUNTERCLOCKWISE TRAVELING DIRECTION: NODE VISITED ALONG THE PATH, ARRIVAL TIME AT EACH NODE, STARTING ENERGY OF EACH NODE IN A RENEWABLE CYCLE, AND CHARGING TIME AT EACH NODE FOR THE 50-NODE NETWORK

Node Order	a_i (s)	E_i (J)	τ_i (s)	Node Order	a_i (s)	E_i (J)	τ_i (s)
42	110702	10747	11	2	117778	10611	41
41	110725	10613	37	44	117848	10605	42
46	110777	9282	305	23	117903	10793	2
28	111113	7697	627	15	117923	10747	11
8	111776	7590	653	25	117960	10685	25
48	112461	714	2092	21	118002	10593	44
43	114579	10594	43	37	118065	8827	425
31	114660	6233	957	29	118519	8493	499
26	115627	10752	10	14	119056	10299	109
50	115639	9851	199	47	119192	10581	47
36	115855	10137	139	17	119246	9246	338
1	115997	9594	254	33	119614	4961	1287
27	116273	10551	53	38	120936	10059	164
5	116353	10646	33	7	121142	10754	10
49	116412	10610	40	45	121171	10658	31
19	116484	10660	29	16	121213	10738	14
18	116538	10622	38	35	121239	10259	120
4	116581	10329	100	32	121380	8628	483
10	116696	10596	43	11	121894	10010	176
24	116747	9648	245	3	122090	6697	924
20	116997	10773	6	40	123039	10790	2
12	117006	10794	1	34	123046	10747	12
39	117032	8565	477	6	123073	10519	63
13	117534	10020	167	30	123151	8319	563
9	117717	10613	40	22	123766	5722	1166

TABLE III
CASE OF CLOCKWISE TRAVELING DIRECTION: NODE VISITED ALONG THE PATH, ARRIVAL TIME AT EACH NODE, STARTING ENERGY OF EACH NODE IN A RENEWABLE CYCLE, AND CHARGING TIME AT EACH NODE FOR THE 50-NODE NETWORK

Node Order	a_i (s)	E_i (J)	τ_i (s)	Node Order	a_i (s)	E_i (J)	τ_i (s)
22	110676	5032	1166	9	117852	10613	40
30	111894	8032	563	13	117907	10023	167
6	112472	10489	63	39	118099	8588	477
34	112550	10741	12	12	118601	10795	1
40	112567	10789	2	20	118605	10773	6
3	112594	6301	924	24	118617	9668	245
11	113538	9944	176	10	118868	10600	43
32	113744	8461	483	4	118928	10339	100
35	114250	10222	120	18	119032	10626	38
16	114382	10734	14	19	119095	10664	29
45	114406	10648	31	49	119156	10615	40
7	114456	10751	10	5	119223	10650	33
38	114508	10012	164	27	119283	10558	53
33	114706	4676	1287	1	119357	9632	254
17	116024	9197	338	36	119613	10160	139
47	116368	10575	47	50	119770	9888	199
14	116443	10286	109	26	119972	10754	10
29	116590	8449	499	31	119992	6464	957
37	117118	8809	425	43	120986	10606	43
21	117561	10593	44	48	121056	1526	2092
25	117624	10685	25	8	123180	7927	653
15	117674	10747	11	28	123868	8059	627
23	117703	10793	2	46	124526	9472	305
44	117718	10605	42	41	124846	10637	37
2	117789	10611	41	42	124896	10754	11

By Property 1, we find that there exists an energy bottleneck node in the network with its energy dropping to E_{min} during a renewable energy cycle. This property is confirmed in our numerical results. This bottleneck node is the 48th node, whose energy behavior is shown in Fig. 9.

In Section VI-B, we showed that minimum energy routing may not be optimal for our problem (see Remark 1). This point is confirmed by our numerical results. In Fig. 10, we show that

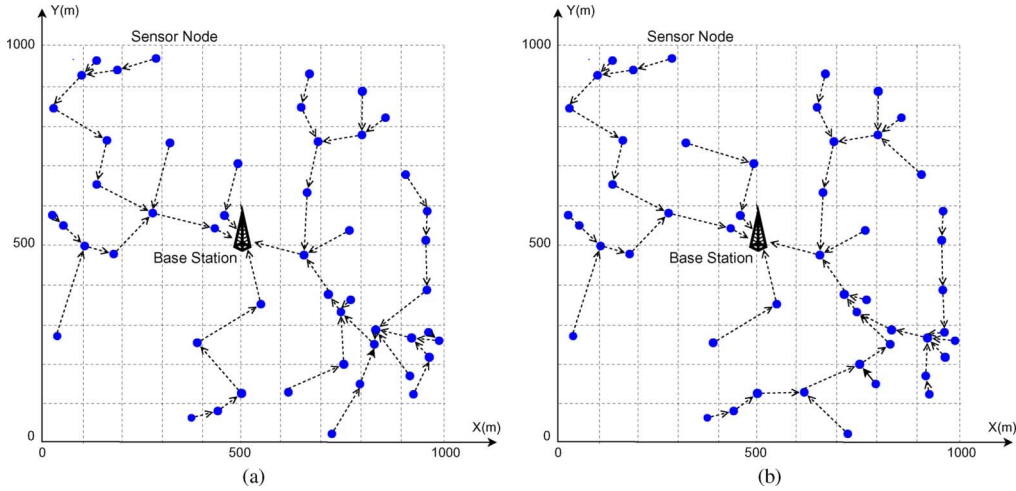


Fig. 10. Comparison of data routing by our solution and that by minimum energy routing for the 50-node network. (a) Data routing in our solution. (b) Minimal energy routing.

TABLE IV
LOCATION AND DATA RATE R_i FOR EACH NODE IN A 100-NODE NETWORK

Node Index	Location (m)	R_i (kb/s)	Node Index	Location (m)	R_i (kb/s)
1	(970, 383)	10	51	(295, 856)	7
2	(124, 85)	8	52	(306, 584)	10
3	(467, 734)	6	53	(106, 374)	8
4	(657, 332)	3	54	(594, 222)	7
5	(290, 840)	3	55	(283, 219)	10
6	(755, 372)	9	56	(155, 522)	1
7	(558, 828)	5	57	(1, 433)	3
8	(428, 177)	9	58	(284, 741)	10
9	(267, 130)	1	59	(551, 70)	8
10	(754, 880)	9	60	(871, 847)	5
11	(898, 44)	1	61	(42, 680)	7
12	(728, 687)	9	62	(905, 137)	5
13	(407, 734)	9	63	(131, 858)	4
14	(938, 437)	6	64	(834, 200)	3
15	(255, 380)	2	65	(800, 607)	4
16	(533, 980)	2	66	(918, 543)	1
17	(955, 399)	8	67	(137, 162)	5
18	(268, 440)	9	68	(505, 6)	4
19	(250, 157)	1	69	(405, 771)	10
20	(928, 326)	8	70	(174, 765)	6
21	(69, 314)	10	71	(575, 421)	9
22	(299, 895)	4	72	(606, 57)	5
23	(592, 247)	7	73	(214, 586)	5
24	(203, 311)	4	74	(520, 174)	9
25	(636, 409)	3	75	(989, 729)	10
26	(798, 708)	8	76	(490, 534)	6
27	(502, 144)	8	77	(695, 253)	10
28	(651, 871)	3	78	(411, 917)	8
29	(796, 83)	6	79	(35, 758)	6
30	(233, 462)	5	80	(293, 887)	10
31	(601, 30)	1	81	(801, 69)	9
32	(112, 753)	1	82	(347, 184)	10
33	(516, 700)	5	83	(83, 737)	7
34	(838, 215)	3	84	(511, 697)	4
35	(921, 680)	4	85	(367, 777)	5
36	(498, 557)	3	86	(739, 502)	10
37	(278, 851)	2	87	(525, 425)	1
38	(653, 559)	4	88	(805, 611)	2
39	(917, 902)	7	89	(817, 856)	5
40	(510, 420)	3	90	(189, 671)	6
41	(974, 358)	7	91	(124, 524)	1
42	(197, 489)	5	92	(821, 299)	7
43	(111, 256)	5	93	(638, 704)	9
44	(297, 929)	2	94	(16, 382)	2
45	(396, 467)	2	95	(896, 568)	5
46	(421, 254)	7	96	(515, 888)	3
47	(311, 431)	3	97	(545, 843)	10
48	(694, 703)	6	98	(606, 899)	7
49	(92, 402)	10	99	(760, 939)	3
50	(402, 182)	8	100	(855, 815)	2

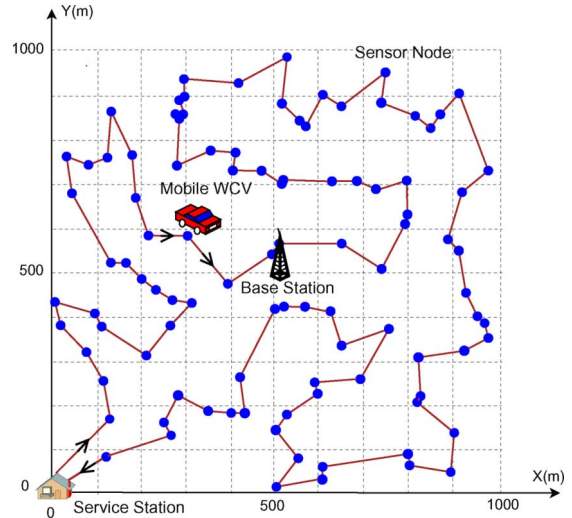


Fig. 11. Optimal traveling path for the WCV for the 100-node sensor network, assuming traveling direction is clockwise.

data routing in our solution differs from the minimum-energy routing for the 50-node network.

100-Node Network: Table IV gives the location of each node and its data rate for a 100-node network. The shortest Hamiltonian cycle is shown in Fig. 11. For this optimal cycle, $D_{TSP} = 7687$ m and $\tau_{TSP} = 1537.4$ s. For the target $\epsilon = 0.01$, by Theorem 2, we have

$$\begin{aligned}
 m &= \left\lceil \sqrt{\frac{U\tau_{TSP}}{4\epsilon(E_{\max} - E_{\min})}} \right\rceil \\
 &= \left\lceil \sqrt{\frac{5 \times 1537.4}{4 \times 0.01 \times (10800 - 540)}} \right\rceil = 5.
 \end{aligned}$$

The solution for the 100-node network includes the cycle time $\tau = 58.52$ h, the vacation time $\tau_{vac} = 50.30$ h, and the objective $\eta_{vac} = 85.95\%$. Additional results are shown in Table V.

TABLE V

CASE OF CLOCKWISE TRAVELING DIRECTION: NODE VISITED ALONG THE PATH, ARRIVAL TIME AT EACH NODE, STARTING ENERGY OF EACH NODE IN A RENEWABLE CYCLE, AND CHARGING TIME AT EACH NODE FOR THE 100-NODE NETWORK

Node Order	a_i (s)	E_i (J)	τ_i (s)	Node Order	a_i (s)	E_i (J)	τ_i (s)
67	210727	10257	109	96	227822	10722	17
43	210855	9254	310	97	227850	9391	307
21	211179	10623	35	7	228162	7595	702
94	211232	10625	35	98	228880	10638	35
57	211278	10762	8	28	228926	9893	199
49	211305	10692	22	99	229151	10762	8
53	211333	9279	306	10	229171	10075	159
24	211661	8065	551	89	229344	10726	16
15	212230	8467	471	100	229371	9797	220
47	212716	4983	1181	60	229599	10613	41
18	213906	10698	21	39	229654	10687	25
30	213935	9012	364	75	229716	10581	48
42	214308	9784	207	35	229781	9415	305
56	214526	10787	3	95	230109	10561	53
91	214534	10778	4	66	230168	10790	2
61	214574	10682	24	14	230192	10720	18
79	214614	10681	24	17	230218	10723	17
83	214649	10274	107	1	230240	10287	113
32	214762	10365	89	41	230358	10716	19
63	214873	10640	33	20	230388	8701	464
70	214926	9839	196	92	230874	7791	668
90	215141	9489	268	34	231559	10732	15
73	215427	8932	383	64	231577	9786	225
52	215828	9431	281	62	231822	10614	41
45	216139	1745	1876	11	231882	10772	6
76	218038	10737	13	81	231908	10715	19
36	218056	7075	775	29	231930	9728	239
38	218862	10152	135	72	232207	10740	13
86	219018	4116	1402	31	232226	10786	3
65	220444	8386	508	68	232249	10724	17
88	220952	9402	294	59	232281	10261	120
26	221266	9845	201	27	232419	10221	129
12	221482	10546	54	74	232556	8179	587
48	221543	10725	16	54	233160	10733	15
93	221570	9030	374	23	233180	7167	817
33	221969	1095	2072	77	234018	10563	53
84	224042	1197	2072	6	234098	6861	890
3	226126	8828	427	4	235009	6073	1075
13	226565	9705	237	25	236100	5792	1146
69	226809	10424	82	71	237259	6167	1066
85	226899	9884	199	87	238335	4268	1516
58	227115	10534	58	40	239855	10743	13
5	227193	9991	176	46	239906	10677	28
37	227372	10781	4	8	239950	10321	111
51	227380	10397	88	50	240066	10481	74
80	227473	10691	24	82	240152	10643	37
22	227499	10752	11	55	240203	9350	338
44	227517	10766	7	19	240555	10785	3
78	227547	9805	217	9	240564	10775	6
16	227791	10742	13	2	240600	10658	33

IX. CONCLUSION

Existing WSNs have been constrained by limited battery energy at a node, and thus finite lifetime is regarded as a fundamental performance bottleneck. This paper has exploited a recent breakthrough in wireless power transfer technology for a WSN and has shown that, once properly designed, a WSN has the potential to remain operational forever. This is the first paper that offers a systematic investigation of a sensor network operating under this new enabling energy transfer technology.

We studied a general scenario where a mobile charging vehicle periodically travels inside the network and charges each sensor node wirelessly without any plugs or wires. We introduced a new concept called renewable energy cycle and offered both necessary and sufficient conditions. We studied a practical optimization problem, with the objective of maximizing

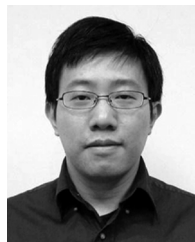
the ratio of the WCV's vacation time over the cycle time. For this problem, we proved that the optimal traveling path for the WCV in each renewable cycle is the shortest Hamiltonian cycle. Subsequently, we developed a provable near-optimal solution for flow routing, total cycle time, and individual charging time at each node. We also showed that traditional minimum energy routing cannot achieve an optimal solution. Using numerical results, we showed the detailed network behavior associated with a renewable energy cycle and demonstrated that a sensor network operating under our solution can indeed remain operational with unlimited lifetime.

There are a number of interesting open questions that deserve further investigation. One important question is scalability, i.e., how does our solution scale when the number of sensor nodes (or density) in the network increases. Interestingly, it has been recently demonstrated by Kurs *et al.* [16] that wireless power transfer can be performed from one energy source node to multiple energy-receiving nodes at the same time. This suggests that the WCV can charge multiple nodes simultaneously on its traveling path and thus has the potential to work in a densely deployed sensor network. We will explore how this technology can address the scalability problem in our future research.

REFERENCES

- [1] Y. Ammar, A. Buhig, M. Marzencki, B. Charlot, S. Basrou, K. Matou, and M. Renaudin, "Wireless sensor network node with asynchronous architecture and vibration harvesting micro power generator," in *Proc. Joint Conf. Smart Objects Ambient Intell., Innov. Context-Aware Services, Usages Technol.*, Grenoble, France, Oct. 12–14, 2005, pp. 287–292.
- [2] *Wireless Sensor Networks: A Systems Perspective*, N. Bulusu and S. Jha, Eds. Norwood, MA: Artech House, 2005, ch. 9.
- [3] J. Chang and L. Tassiulas, "Maximum lifetime routing in wireless sensor networks," *IEEE/ACM Trans. Netw.*, vol. 12, no. 4, pp. 609–619, Aug. 2004.
- [4] Concorde, "Concorde TSP Solver," 2011 [Online]. Available: <http://www.tsp.gatech.edu/concorde/>
- [5] I. Dietrich and F. Dressler, "On the lifetime of wireless sensor networks," *Trans. Sensor Netw.*, vol. 5, no. 1, pp. 1–39, Feb. 2009.
- [6] A. Giridhar and P. R. Kumar, "Maximizing the functional lifetime of sensor networks," in *Proc. ACM/IEEE Int. Symp. Inf. Process. Sensor Netw.*, Los Angeles, CA, Apr. 2005, pp. 5–12.
- [7] E. Giler, "Eric Giler demos wireless electricity," 2009 [Online]. Available: http://www.ted.com/talks/eric_giler_demos_wireless_electricity.html
- [8] S. He, J. Chen, F. Jiang, D. K. Y. Yau, G. Xing, and Y. Sun, "Energy provisioning in wireless rechargeable sensor networks," in *Proc. IEEE INFOCOM*, Shanghai, China, Apr. 2011, pp. 2006–2014.
- [9] W. B. Heinzelman, "Application-specific protocol architectures for wireless networks," Ph.D. dissertation, Dept. Elect. Eng. Comput. Sci., MIT, Cambridge, MA, 2000.
- [10] Y. T. Hou, Y. Shi, and H. D. Sherali, "Rate allocation and network lifetime problems for wireless sensor networks," *IEEE/ACM Trans. Netw.*, vol. 16, no. 2, pp. 321–334, Apr. 2008.
- [11] IBM, "IBM ILOG CPLEX optimizer," 2011 [Online]. Available: <http://www-01.ibm.com/software/integration/optimization/cplex-optimizer/>
- [12] X. Jiang, J. Polastre, and D. Culler, "Perpetual environmentally powered sensor networks," in *Proc. ACM/IEEE Int. Symp. Inf. Process. Sensor Netw.*, Los Angeles, CA, Apr. 2005, pp. 463–468.
- [13] S. Jain, K. Fall, and R. Patra, "Routing in a delay tolerant network," in *Proc. ACM SIGCOMM*, Portland, OR, 2004, pp. 145–158.
- [14] A. Kansal, J. Hsu, S. Zahedi, and M. B. Srivastava, "Power management in energy harvesting sensor networks," *Trans. Embed. Comput. Syst.*, vol. 6, no. 4, Article 32, Sep. 2007.
- [15] A. Kurs, A. Karalis, R. Moffatt, J. D. Joannopoulos, P. Fisher, and M. Soljacic, "Wireless power transfer via strongly coupled magnetic resonances," *Science*, vol. 317, no. 5834, pp. 83–86, 2007.
- [16] A. Kurs, R. Moffatt, and M. Soljacic, "Simultaneous mid-range power transfer to multiple devices," *Appl. Phys. Lett.*, vol. 96, no. 4, Article 4102, Jan. 2010.

- [17] Z. Li, Y. Peng, W. Zhang, and D. Qiao, "J-RoC: A joint routing and charging scheme to prolong sensor network lifetime," in *Proc. IEEE ICNP*, Vancouver, BC, Canada, Oct. 17–20, 2011, pp. 373–382.
- [18] S. Meninger, J. O. Mur-Miranda, R. Amirtharajah, A. P. Chandrakasan, and J. H. Lang, "Vibration-to-electric energy conversion," *IEEE Trans. Very Large Scale Integr. (VLSI) Syst.*, vol. 9, no. 1, pp. 64–76, Feb. 2001.
- [19] *Handbook of Batteries*, D. Linden and T. B. Reddy, Eds., 3rd ed. New York: McGraw-Hill, 2002, ch. 1.
- [20] M. Padberg and G. Rinaldi, "A branch-and-cut algorithm for the resolution of large-scale symmetric traveling salesman problems," *SIAM Rev.*, vol. 33, no. 1, pp. 60–100, 1991.
- [21] G. Park, T. Rosing, M. D. Todd, C. R. Farrar, and W. Hodgkiss, "Energy harvesting for structural health monitoring sensor networks," *J. Infrastruct. Syst.*, vol. 14, no. 1, pp. 64–79, Mar. 2008.
- [22] Y. Peng, Z. Li, W. Zhang, and D. Qiao, "Prolonging sensor network lifetime through wireless charging," in *Proc. IEEE RTSS*, San Diego, CA, 2010, pp. 129–139.
- [23] Powercast, "PowerCast," [Online]. Available: <http://www.powercastco.com>
- [24] A. Sankar and Z. Liu, "Maximum lifetime routing in wireless ad-hoc networks," in *Proc. IEEE INFOCOM*, Hong Kong, Mar. 7–11, 2004, pp. 1089–1097.
- [25] R. C. Shah, S. Roy, S. Jain, and W. Brunette, "Data MULEs: Modeling a three-tier architecture for sparse sensor networks," in *Proc. 1st IEEE SNPA*, Anchorage, AK, May 2003, pp. 30–41.
- [26] Y. Shi and Y. T. Hou, "Theoretical results on base station movement problem for sensor network," in *Proc. IEEE INFOCOM*, Phoenix, AZ, Apr. 2008, pp. 376–384.
- [27] Y. Shi, L. Xie, Y. T. Hou, and H. D. Sherali, "On renewable sensor networks with wireless energy transfer," Bradley Department of Electrical and Computer Engineering, Virginia Tech, Blacksburg, VA, Tech. Rep., 2010 [Online]. Available: <http://filebox.vt.edu/users/windgoon/papers/charging.pdf>
- [28] N. Tesla, "Apparatus for transmitting electrical energy," US Patent no. 1,119,732, Dec. 1914.
- [29] B. Tong, Z. Li, G. Wang, and W. Zhang, "How wireless power charging technology affects sensor network deployment and routing," in *Proc. IEEE ICDCS*, Genoa, Italy, Jun. 2010, pp. 438–447.
- [30] T. A. Vanderelli, J. G. Shearer, and J. R. Shearer, "Method and apparatus for a wireless power supply," US Patent no. 7,027,311, Apr. 2006.
- [31] W. Wang, V. Srinivasan, and K. C. Chua, "Extending the lifetime of wireless sensor networks through mobile relays," *IEEE/ACM Trans. Netw.*, vol. 16, no. 5, pp. 1108–1120, Oct. 2008.
- [32] WiTricity, "WiTricity Corp.," 2011 [Online]. Available: <http://www.witricity.com>
- [33] Wireless Power Consortium, "Wireless Power Consortium," 2008 [Online]. Available: <http://www.wirelesspowerconsortium.com/>
- [34] F. Zhang, X. Liu, S. A. Hackworth, R. J. Scabassi, and M. Sun, "In vitro and in vivo studies on wireless powering of medical sensors and implantable devices," in *Proc. IEEE/NIH LiSSA*, Bethesda, MD, Apr. 2009, pp. 84–87.
- [35] W. Zhao, M. Ammar, and E. Zegura, "A message ferrying approach for data delivery in sparse mobile ad hoc networks," in *Proc. ACM MobiHoc*, Tokyo, Japan, May 2004, pp. 187–198.



Liguang Xie (S'08) received the B.S. degree in computer science from Zhejiang University, Hangzhou, China, in 2006, and the M.S. degree in computer science from Virginia Tech, Blacksburg, in 2009, and is currently pursuing the Ph.D. degree in computer engineering at Virginia Tech.

His research interests include optimization and algorithm design for wireless networks, with a current focus on wireless power transfer for energy-constrained wireless networks.



Yi Shi (S'02–M'08) received the Ph.D. degree in computer engineering from Virginia Tech, Blacksburg, in 2007.

He is currently an Adjunct Assistant Professor with the Bradley Department of Electrical and Computer Engineering, Virginia Tech. His research focuses on algorithms and optimization for cognitive radio networks, MIMO and cooperative communication networks, sensor networks, and ad hoc networks.

Dr. Shi was a recipient of the IEEE INFOCOM 2008 Best Paper Award and the only Best Paper

Award Runner-Up of IEEE INFOCOM 2011.



Y. Thomas Hou (S'91–M'98–SM'04) received the Ph.D. degree in electrical engineering from the Polytechnic Institute of New York University, Brooklyn, in 1998.

From 1997 to 2002, he was a Researcher with Fujitsu Laboratories of America, Sunnyvale, CA. Since 2002, he has been with the Bradley Department of Electrical and Computer Engineering, Virginia Tech, Blacksburg, where he is now an Associate Professor. His research interests are cross-layer optimization for cognitive radio wireless networks, cooperative communications, MIMO-based ad hoc networks, and new interference management schemes for wireless networks.



Hanif D. Sherali is a University Distinguished Professor and the W. Thomas Rice Chaired Professor of Engineering with the Grado Department of Industrial and Systems Engineering, Virginia Tech, Blacksburg. His areas of research interest are in analyzing problems and designing algorithms for specially structured linear, nonlinear, and integer programs arising in various applications, global optimization methods for nonconvex programming problems, location and transportation theory and applications, and economic and energy mathematical

modeling and analysis.

Prof. Sherali is an elected member of the U.S. National Academy of Engineering.